Order Number 9405534

Evidence for an actomyosin system in *Tetrahymena*

Hoey, John Gabriel, Ph.D.

City University of New York, 1993

U·M·I
300 N. Zeeb Rd.
Ann Arbor, MI 48106

Evidence for an Actomyosin System in *Tetrahymena*

by

John G. Hoey

A dissertation submitted to the Graduate Faculty in Biology in partial fulfillment of the requirements for the degree of Doctor of Philosophy, The City University of New York

1993

This manuscript has been read and accepted for the Graduate Faculty in Biology in satisfaction of the dissertation requirement for the degree of Doctor of Philosophy.

Sept. 10, 1993
Date

Chairman of Examining Committee
Dr. Ray H. Gavin, Brooklyn College

September 10, 1993
Date

Executive Officer
Dr. Richard L. Chappell

Dr. Charlene Forest, Brooklyn College

Dr. J. R. Collier, Brooklyn College

Dr. William D. Cohen, Hunter College

Dr. Linda A. Hufnagel, University of Rhode Island

Supervising Committee

The City University of New York

Abstract

Evidence for an Actomyosin System in *Tetrahymena*

by

John G. Hoey

Advisor: Dr. Ray H. Gavin

Affinity-purified antibodies were used in conjunction with immunofluorescence and immunogold microscopy to study the distribution of actin in *Tetrahymena* and to provide evidence for a putative actomyosin system in this organism. An antiserum against a *Tetrahymena* oral apparatus fraction enriched for basal body proteins was produced in rabbits. Agarose-linked muscle actin was used to affinity-purify anti-*Tetrahymena* actin antibodies from the oral apparatus antiserum. The affinity-purified antibodies were monospecific for *Tetrahymena* actin on immunoblots containing total oral apparatus protein. Agarose-linked myosin II light chains were used to affinity-purify antibodies that detected an 18 kDa *Tetrahymena* polypeptide on immunoblots but did not cross react with actin. With immunofluorescence microscopy, the anti-actin antibodies localized to basal bodies in *Tetrahymena*. *Tetrahymena* basal bodies are contained within separate, filamentous cages which are closely associated with basal body microtubules. At the ultrastructural level with the immunogold labeling technique, the affinity-purified, anti-actin antibodies labeled actin epitopes in four distinct regions of the basal body-cage complex: (a) basal

body walls, (b) basal plate filaments, (c) proximal-end filaments, and (d) cage wall filaments. The anti-actin antibodies also localized to mucocysts (cortical secretory organelles), and to the fibrillar macronuclear matrix. Quantitative analysis of gold particle distribution was used to demonstrate the specificity of the antibodies for the basal body-cage complex, mucocysts, and macronuclear matrix and to show that non-specific binding of the antibodies was negligible. Preadsorption of the antibody with muscle actin effectively eliminated the capacity of the antibody to bind to proteins on immunoblots and to basal body structures with the immunogold labeling technique. The anti-18 kDa antibody and the anti-actin antibody co-localized to components of the basal body-cage complex. A *Tetrahymena* cortical fraction containing basal bodies exhibited both Mg^{2+}-EGTA and K^{+}-EDTA ATPase activity. Approximately 60% of the Mg^{2+}-EGTA ATPase activity was vanadate-insensitive. The data in this study provide evidence for an actomyosin system in *Tetrahymena* which could play a role in basal body movement and in the discharge of mucocyst contents.

ACKNOWLEDGEMENTS

The author would like to dedicate this work to the following persons, without whose help this work could never have been brought to fruition.

To:

Dr. R. H. Gavin-- My mentor, friend, and colleague. For those many years of tireless patience, dedication, and inspiration. All that I have become or will ever achieve, I owe to you. Your unwavering support and encouragement have set me on the path to success. Thank you so much.

Mark and Iris--My best friends. For those countless hours of quiet counsel. Your advice, wisdom, and inspiration have strenghtened me throughout this endeavor. You have been there virtually every step of the way, and I thank the both of you for your honest, pragmatic approach to every conversation that we have shared.

Mom and Dad--For instilling in me the self-confidence and determination to overcome the hurdles. I thank the both of you for being there when I needed you.

L. A. H.--I will forever cherish the memories of you and all that you have done to make this journey a little easier. Thanks for your support and understanding.

TABLE OF CONTENTS

LIST OF TABLES PAGE

LIST OF FIGURES PAGE

INTRODUCTION

The evolution of cellular machinery for transducing the chemical energy present in triphosphate nucleotides into mechanical energy capable of mediating coordinated movement was a significant turning point in the lineage of eukaryotic organisms. It afforded early eukaryotes the opportunity for adaptation and survival under a variety of selective pressures. The ability to respond and react to external and internal stimuli was significantly enhanced by the development of force-generating elements able to carry out contraction and elongation of fibrous elements in response to changes in the surrounding milieu. Represented by a diverse group of molecules and mechanisms, force-generating or contractile systems have been identified in every eukaryotic organism in which their existence has been sought.

Actin and Myosin - An Historical Overview

In tracing the historical literature on contractile systems, one is perhaps not surprised to learn that the earliest thoughts on this subject are credited to the Greek philosophers and physicians of antiquity. Their prolific discourses on muscle movement were nothing short of astute (reviewed by Fulton, 1926 and Needham, 1971). The intense interest in the structural and chemical nature of muscle that began about 500 B. C. was to continue almost unabated for well over two millenia. It was not, however, until the latter part of the 19th century, with the discovery of myosin, that the major contractile proteins began to be identified and characterized.

W. Kuhne's description of the preparation of myosin, published in 1864, was a landmark event in the historical development of contractile systems (reviewed by Needham, 1971). His procedure for the isolation of myosin, involved the pulverization of frozen isolated frog muscle. Upon thawing, this material assumed a liquid "syrupy" state that could readily be filtered (Needham, 1971). When this material was subsequently dropped into water, a white precipitate was formed which could be redissolved if the ionic strength of the mixture was raised. Moreover, if dilute HCl was used in lieu of H_2O, a salt-insoluble precipitate formed immediately but readily redissolved. This liquid could be kept at 0°C but formed a "coagulum" at warmer temperatures. Kuhne called this coagulated mass, *myosin* (Needham, 1971).

Halliburton (1887) used Kuhne's procedure to isolate mammalian muscle myosin. He further investigated the temperature-induced coagulation of myosin and several other muscle protein fractions (Halliburton, 1887). He also made attempts to isolate some of the muscle proteins taking advantage of their coagulation properties (Halliburton, 1887). Halliburton identified two proteins from the myosin fraction that differed with respect to the temperature at which they precipitated. The first protein, called *paramyosinogen*, could be precipitated at 47°C (Halliburton, 1887). The second protein precipitated at 56°C or under higher ionic conditions than the first. He called this protein *myosinogen* (Halliburton, 1887).

Halliburton went on to analyze the coagulation properties of these two proteins, later contending "that he had evidence for the participation in the gelation process of a 'myosin ferment' analogous to the fibrin-ferment in blood clotting" (Halliburton, 1887). The preparation of this ferment entailed

the treatment of isolated muscle with alcohol, followed by drying to a powder over sulphuric acid. This powder could be solubilized in water. When aqueous extracts of the powder were added to a solution of myosin, there was an observable enhancement of its coagulation (Halliburton, 1887). The properties ascribed by Halliburton to this muscle preparation are strikingly similar to those of the second major contractile protein, actin.

The work of Huxley (1902) provided the first detailed description of the organization of muscle tissue using crayfish muscle as a model system. He described muscle fibers as consisting of a series of dark transverse lines, termed septa, located at intervals of 1/4000th of an inch (Huxley, 1902). On either side of each septal line there was a transparent band called the septal zone followed by a broad dark region referred to as the interseptal zone (Huxley, 1902). The inter-septal zones polarized light, whereas the septa did not (Huxley, 1902). Thus, in the darkfield of the polarizing microscope, the dark septa appeared to be crossed by bright intersepta bands (Huxley, 1902). In muscle which had been extracted with strong acids to solubilize myosin, the inter-septal zones lost their polarizing property.

Continuing with the historical background on myosin, we turn now to the work of H. H. Weber who, in 1925, carried out a detailed biochemical analysis of myosin and other muscle proteins (reviewed by Needham, 1971 and Mommaerts, 1992). He determined the isoelectric point of myosin to be at pH 5.2, and that of myosinogen at pH 6.3. Needham (1971) points out that the protein originally given the name *myosinogen* by Halliburton had subsequently been renamed *myogen* by von Furth in 1925. Von Furth justified the renaming of myosinogen by citing his own experimental evidence suggesting that this protein was not a globulin as myosin was and therefore could not be a precursor of myosin (Needham, 1971).

Weber's major contribution, according to Mommaerts (1992), was his "preparation of myosin threads". This was achieved by forcing a solution of myosin through a narrow tube into a low-salt solution, forming a precipitate of threads (Mommaerts, 1992) whose meager birefringence could be amplified by "stretching and drying" (Needham, 1971).

Szent-Gyorgyi (1948) had taken an intense interest in the ATP-induced drop in viscosity of a myosin solution derived from a high salt muscle extract. Apparently, he had become interested in the difference in properties between the two different forms of myosin, known at the time as myosins A and B for the low and high viscosity forms of this enzyme, respectively (Szent-Gyorgyi, 1948). The low viscosity form of myosin had been derived from a 20 minute extraction of muscle in a high salt solution, whereas the high viscosity form had been derived from a 24 hour extraction in the same solution (Szent-Gyorgyi, 1948).

Szent-Gyorgyi conducted experiments in which he studied the effect of ATP on myosins A and B. He observed that myosin B threads could be induced to contract if they were suspended in an aqueous extract of muscle (Szent-Gyorgyi, 1948). Furthermore, overnight storage of this extract led to the disappearance of this contractile behavior. If ATP and certain ions such as K^+ and Mg^{2+} were then added to the mixture, contraction could once again be induced. No contraction was observed when myosin A was treated in an analogous way (Szent-Gyorgyi, 1948).

Elucidation of the fundamental differences between myosin A and B, and the subsequent identification of a new muscle protein known as *actin*, came from the studies of F. Bruno Straub (reviewed by Mommaerts, 1992), who prepared an acetone powder of ground muscle which had previously

been extracted of its myosin. Straub then proceeded to mix this powder with either water or a dilute salt solution. The extract that had been prepared with the water had very low viscosity and "contained a low concentration, less than a percent, of a globular protein" (Mommaerts, 1992). Upon addition of dilute salt, there was a dramatic increase in viscosity and birefringence; these changes occurred over the course of several minutes (Mommaerts, 1992). Conversely, when the acetone powder was treated with the dilute salt solution there was a much more rapid change in viscosity and birefringence. As a result, Straub speculated that this protein could exist in either a globular or fibrous form. He postulated that these two forms were in fact inactive and active states of the same molecule, and that the transition from the former to the latter could be induced by salt (Mommaerts, 1992). Szent-Gyorgyi would later coin the terms G- and F-actin for these two forms, respectively. Both forms of this protein were shown to retain their ability to react with myosin, but only the fibrous form could give rise to myosin B, the highly viscous form of myosin. Straub gave the name *actin* to this myosin *activating protein*, and the term *actomyosin* to the mixture of myosin and the fibrous (F) form of this protein (Mommaerts, 1992).

Biochemistry of Actin and Myosin

Actin

Actin is one of the most abundant eukaryotic proteins, typically constituting 5-15% of the total protein content of a cell (Lackie, 1986). It is a globular protein comprised of 374-375 amino acids (mol. wt. 43 kDa), with an isoelectric point of about 5.5. Over a half century of research on this protein since its identification by Straub, in 1942 (reviewed by Korn, 1982), has led to a staggering amount of literature on its structural, biochemical, and functional properties.

Electron microscopy and 3-dimensional reconstruction have been used to ascertain the structure of pure monomeric actin (Pollard and Cooper, 1986). An electron density map of actin has been obtained from X-ray diffraction analysis of cocrystals of actin and DNase I (Pollard, 1990). These studies have demonstrated that actin exists as a monomeric, dumbbell-shaped molecule consisting of two lobes of unequal size separated by a cleft (Pollard and Cooper, 1986; Bray, 1992a). Evidence has been presented for separate binding sites within the cleft for nucleotides and divalent cations (Jacobsen and Rosenbusch, 1976). If residues 1-68 are proteolytically removed from the actin molecule, the ability of actin to bind divalent cations is lost while the nucleotide-binding affinity is retained (Barden *et al.*, 1980). Although these cation binding sites have affinities for both Ca^{2+} and Mg^{2+}, Ca^{2+}-actin binds ATP much stronger than Mg^{2+}-actin (Korn, 1982). Isolated monomeric skeletal actin has bound to it 1 mol of ATP and 1 mol of Ca^{2+} (Korn, 1982). Removal of the bound ATP can be carried out by prolonged dialysis, but the process can be expedited when the bound Ca^{2+} is removed by EDTA chelation

(Korn, 1982). Removal of the divalent cation and the nucleotide results in denaturation of the actin molecule (Korn, 1982).

In its monomeric form actin is known as globular or G-actin. G-actin is capable under physiological conditions of undergoing polymerization into a filamentous helical polymer. This property, combined with its inherent ability to interact with a score of actin-binding proteins, allows actin to carry out a diverse array of biological activitites such as cytoskeletal organization, cytokinesis, muscle contraction, and phagocytosis. Polymeric actin has an intrinsic polarity which can be revealed when a myosin subfragment, heavy meromyosin (HMM), binds to the filament. The HMM molecules are deposited in an arrowhead configuration, all in the same orientation on the filament, creating a "barbed" end and a "pointed" end.

The transition from globular (G) actin to its filamentous (F) form is initiated by the addition of K^+, Mg^{+2}, or Ca^{+2} ions (Stossel, 1985). *In vitro,* polymerization is correlated with an increase in the viscosity of a solution containing actin. This process can therefore be conveniently followed either by monitoring the increase in viscosity of a solution containing monomeric actin or by direct visualization of actin filaments by electron microscopy. For a comprehensive review of the polymerization process, the reader is referred to Pollard and Cooper (1986).

In general, the polymerization of skeletal muscle actin can be divided into four stages: activation, nucleation, elongation, and annealing (Pollard and Cooper, 1986).

Activation: During this phase, actin monomers undergo a conformational change prior to associating with each other to form polymers. Polymerization can be initiated by K^+, Mg^{2+}, or Ca^{2+} (Neuhaus *et*

al., 1983). However, the conformational change is probably Mg^{2+}-induced (Frieden, 1982). The precise effect of bound cations on actin structure remains controversial (Pollard, 1990).

Nucleation: During this phase, activated actin monomers associate into oligomers. The minimum concentration of monomers required for the initiation of polymerization is referred to as the critical concentration. At this concentration activated monomers spontaneously associate into aggregates called nuclei. The number of nuclei is proportional to the number of actin filaments formed during elongation (Stossel *et al.*, 1985). The seed for the nucleation event is believed to be an actin trimer (Pollard and Cooper, 1986). Because of the inherent thermodynamic instability of actin dimers, nucleation is believed to be the rate-limiting step in the polymerization reaction, and is responsible for the lag-phase observed during in vitro assembly (Pollard and Cooper, 1986).

Elongation: After the lag phase, there is a steady increase in the amount of polymer through the reversible association of actin monomers at either end of the growing filament. The length of the polymer increases until filament and actin monomer concentration reach a dynamic steady state (Stossel *et al.*, 1985). This aspect of the polymerization process can best be understood by considering first the nucleotide-binding capabilities of monomeric actin, and then the rate constants for the two ends of the filament. Actin monomers can bind both ATP and ADP. As discussed by Stossel *et al.*, (1985), polymerization of actin is associated with, but not kinetically linked to, the hydrolysis of ATP bound to monomeric actin. The rate of polymerization is dependent upon which nucleotide, ATP or ADP, is bound to the actin monomers. Actin assembly is promoted by the delay in

the hydrolysis of ATP at the filament ends (Stossel *et al.*, 1985). When the ATP hydrolysis rate lags behind actin polymerization rate, as might be the case when free monomer concentration is very high, actin monomers at the filament ends will have ATP bound to them. Monomers possessing ATP dissociate more slowly from filaments than those containing ADP. This creates an ATP "cap" which retards monomer loss from filament ends (Stossel *et al.*, 1985). As a result, there will be net addition of subunits at the ends of the filaments. As monomers become incorporated into the growing filament, the free monomer concentration decreases. The net result is that ATP-actin at the filament ends will be hydrolyzed at a faster rate than monomer addition to the filament ends, creating ADP-actin at filament ends. Because the rate of filament polymerization is much slower when ADP-actin is associated with filament ends, there will be a net dissociation of actin monomers from the filament ends (Stossel *et al.*, 1985) under conditions of low monomer concentration. At steady state, the concentration of monomers is different at the two ends of the filament. The critical monomer concentration at the (+) end is an order of magnitude lower than the critical monomer concentration at the (-) end (Stossel *et al.*, 1985). This imbalance in concentration leads to preferential assembly at the barbed (+) end, and preferential dissassembly at the pointed (-) end.

Annealing: Two actin fllaments can be joined in an end-to-end association. This would presumably be facilitated by any of several actin filament-bundling proteins such as caldesmon, alpha-actinin, band 4.9, or fimbrin (Pollard and Cooper, 1986).

Higher eukaryotes possess multiple actin isoforms encoded for by a family of actin genes. The existence of multiple forms of actin has been confirmed by several investigators (Garrels and Gibson, 1976; Rubenstein and Spudich, 1977). Using high resolution two-dimensional polyacrylamide gel electrophoresis (PAGE), Garrels and Gibson (1976) identified three isoforms of rat skeletal muscle actin, designated alpha, beta, and gamma actin. These authors used tryptic digests to determine the relationship of these three actins with each other and with purified muscle actin. Peptide maps generated from digests of the three putative actins indicated that these polypeptides were indeed distinct isoforms of actin. Moreover, there was a differential distribution of these actins among numerous muscle and non-muscle animal cell lines including kidney, brain, and liver.

Actin is one of the most evolutionarily conserved proteins. There is only ≈ 8% difference in primary structure between actin from the slime mold *Physarum polyencephalum* and skeletal muscle (See Korn, 1982 for review). Moreover, there is only ≈ 5% sequence difference between actin from this slime mold and mammalian nonmuscle actins (Korn, 1982).

Pollard and Cooper (1986) suggest that, based on amino acid sequence homologies, protozoan and fungal cytoplasmic actins are the forebearers of all animal actins except vertebrate muscle actins. The latter appear to represent a separate family whose actins make up the structural backbone of skeletal, smooth, and cardiac muscle. It is worth noting that there are definite tissue-specific residues. This specificity is most notable in the first 17 residues at the NH_2-terminus (Korn, 1982). The extraordinary degree of amino acid conservation among the various actins "argues strongly that most residues of actin are involved in specific essential interactions" (Korn, 1982).

Myosins

Myosins are force-generating enzymes capable of transmuting the chemical energy harbored in ATP into the mechanical energy needed to support movement along actin filaments (reviewed by Kiehart, 1990). These are multimeric proteins consisting of a globular head domain fused to a variable tail domain. It is the relatively conserved head domain that possesses ATPase activity, undergoing a conformational change in the presence of actin and ATP to generate force. Kiehart (1990), notes that the variable nature of the tail region allows myosin to be "customized" for powering a wide variety of movements. Myosins can be broadly grouped into two major classes: myosins I and myosins II. This classification is based on the number of heavy chains present.

Myosin II

Myosin II, also known as conventional myosin, is present in vertebrate skeletal muscle where it comprises the thick filaments. It is also a feature of many nonmuscle cells. These are heximeric molecules composed of one pair of heavy chains (mol. wt. 200 kDa) and two pairs of nonidentical light chains (mol. wt. 16-25 kDa). The NH_2-terminus of each heavy chain is folded into a globular head domain that is 17-20 nm long (Cooke, 1986). Each head binds one member of each nonidentical pair of light chains (Lowey *et al.*, 1969). The carboxy-termini of the two globular heavy chains are intertwined into an alpha-helical coiled-coil tail domain (Lowey *et al.*, 1969; Kiehart, 1990; Maita *et al.*, 1991).

There are two flexible portions of the myosin molecule: a hinge-like region in the tail domain, and a swivel section located between the head and

rod domains. Cooke (1986) reviewed the structural basis and functional ramifications of these two flexible regions. The flexible hinge and swivel domains are particularly susceptible to proteolysis. Incubation of myosin with proteases such as trypsin or papain results in the cleavage of the myosin molecule into two fragments--heavy meromyosin (HMM) and light meromyosin (LMM) (Lowey *et al.*, 1969). The HMM fraction consists of the globular heads with their associated light chains. The LMM component consists of the myosin tails (Lowey *et al.*, 1969). Subfragment 1 (S_1) is another product of limited proteolysis of the myosin molecule. This fragment consists of a single globular head with associated light chains (Lowey *et al.*, 1969). Both HMM and S_1 retain the ATPase and actin-binding properties of the native myosin molecule (Lowey *et al.*, 1969).

Myosin II molecules spontaneously associate in a tail-to-tail fashion to make up thick filaments (Cooke, 1986). Thick filaments are bipolar; the myosin heads within each half of a filament face away from the filament's center. This leaves a bare zone in the center of the filament which is devoid of heads.

The myosin head is responsible for ATP hydrolysis and for binding to actin filaments. The globular head of each heavy chain contains one ATP-binding site and one actin-binding site. The ATP-binding site is located near the amino terminus (Korn and Hammer, 1990). For *Acanthamoeba* myosin II, this site corresponds to an amino acid approximately 11 kDa from the amino terminus (reviewed by Korn and Hammer, 1990). The actin-binding domain is located near the flexible neck separating the head and tail domains in each heavy chain (Kiehart, 1990).

When myosin heads are incubated with ATP, the rate of ATP hydrolysis

is slow; each myosin head splits an ATP molecule about once every thirty seconds. However, in the presence of actin filaments, the rate of ATP hydrolysis is enhanced approximately 200-fold. This enhancement of myosin ATP hydrolysis in the presence of filamentous actin is known as the *actin-activated* ATPase activity of myosin.

The physical and chemical properties of the light chains from myosin II have been extensively characterized. SDS PAGE of myosin isolated from fast skeletal muscle reveals three low molecular weight polypeptides of 25, 18, and 16 kDa (Weeds, 1969; Weeds and Lowey, 1971; Lowey and Holt, 1971). Amino acid composition analysis of these three polypeptides shows that the 25 kDa and the 16 kDa components are related, whereas the 18 kDa is chemically different. The physical and chemical unrelatedness of the 18 kDa to the other two light chains is further exemplified by the treatment required to remove these light chains from the myosin molecule. Dissociation of the 18 kDa polypeptide from myosin can be readily acheived using sulfhydryl reagents such as 5, 5'-dithio-bis-2-nitrobenzoic acid (DTNB) (Weeds, 1969; Lowey and Holt, 1971). On the other hand, removal of the 25 and 16 kDa components requires titration to an extremely basic pH (Lowey and Holt, 1971). Hence, the 16 and 25 kDa light chains are known as *alkali* light chains. Removal of the 18 kDa light chain from skeletal muscle myosin does not alter the ATPase activity of the enzyme, suggesting that the 18 kDa light chain is not essential for this activity (Lowey and Holt, 1971). In contrast, neither the 16 nor the 25 kDa component can be removed without total loss of ATPase activity (Lowey and Holt, 1971).

Myosin I

Myosins I belong to a family of myosins that were discovered twenty years ago by Pollard and Korn (1973). These are single-headed myosins with short, inconspicuous tails. There is at least one light chain associated with the heavy chain (Korn *et al.*, 1988). The absence of a rodlike tail domain confers upon these molecules one of their most distinguishing properties, the inability to form bipolar filaments. All available evidence indicates that these myosins are associated exclusively with cellular membranes (reviewed by Pollard *et al.*, (1991).

Myosins I appear to be present in virtually all eukaryotic organisms (Pollard *et al.*, 1991). Three myosin I isoforms, designated myosins IA, IB, and IC, have been identified and characterized in the protozoan *Acanthamoeba castellanii.* Myosin IA possesses a heavy chain of 140 kDa and a light chain of 17 kDa. Myosin IB has a heavy chain of mol. wt. 125 kDa with a single light chain of 27 kDa, while myosin IC possesses a heavy chain of 130 kDa and two light chains of 14 kDa each (Korn *et al.*, 1988; Baines *et al.*, 1992). The slime mold *Dictyostelium* possesses at least one myosin I, and the avian intestinal brush border contains a 110 kDa myosin with calmodulin-like light chains (reviewed by Cheney and Mooseker, 1992). Although these five myosins I are by far the best characterized members of this family, evidence is beginning to confirm the presence of myosin I in humans (Carboni *et al.*, 1988), and even in higher plants (Vahey *et al.*, 1982).

The primary structures of at least ten myosin I heavy chains have been determined. These studies demonstrate that there is a highly conserved head domain and a somewhat variable tail region (Pollard *et al.*, 1991). The highly conserved residues of the myosin I head are virtually homologous to the head sequences of myosin II (Pollard *et al.*, 1991). There is a sequence of highly

conserved residues close to position 400. This sequence apparently distinguishes most known myosins-I from myosins-II (Pollard *et al.*, 1991).

The myosins I of *Acanthamoeba* contain two actin-binding sites. There is an ATP-sensitive actin-binding site within the head of the heavy chain. In the presence of ATP, myosin I heads bind to actin filaments with much lower affinities than for myosin heads in the absence of ATP (Pollard *et al.*, 1991). The latter state is analogous to the rigor state of skeletal muscle (Pollard *et al.*, 1991). The second actin-binding site is ATP-insensitive (Pollard *et al.*, 1991; Korn and Hammer, 1990) and is located in the carboxy terminus of the heavy chain (Korn and Hammer, 1990). Presumably, the second actin-binding site confers upon myosin I the ability to cross-link actin filaments (Korn and Hammer, 1990).

Myosin I tails lack the alpha-helical coiled-coil structure that is a conspicuous feature of conventional myosins (Jung *et al.*, 1987). Furthermore, these tails possess a stretch of 180-250 amino acids with a net positive charge (Pollard *et al.*, 1991). In addition, most of the amoeboid myosins I possess a motif that is rich in glycine, proline, and alanine. As a result, this region is known as the GPA domain.

That myosins I are associated almost exclusively with cell membranes has been demonstrated using immunofluorescence microscopy in conjunction with polyclonal antibodies (Gadasi and Korn, 1980). Additional supportive evidence for plasma membrane association of *Acanthamoeba* myosin I was provided by Adams and Pollard (1989), who demonstrated the binding of myosin I to purified NaOH-extracted plasma membranes. Additionally, immunogold electron microscopy has been used to show that *Acanthamoeba* myosin IA and IB localize primarily to cellular membranes of

vegetative and phagocytosing cells (Baines *et al.*, 1992). Myosin IC, in addition to a plasma membrane association, is also localized to contractile vacuole membranes (Baines and Korn, 1990).

The actin activated Mg^{2+}-ATPase activity of myosin I from *Acanthamoeba* is fully expressed when a single residue within the heavy chain is phosphorylated by a myosin I heavy chain kinase (HCK) (Maruta and Korn, 1977). This kinase has been partially purified (Hammer *et al.*, 1983) and its substrate specificities determined (Brzeska *et al.*, 1990a). In addition, myosin I HCK has been localized to *in situ* cell membranes and to purified plasma membranes (Kulesza-Lipka *et al.*, 1991). Myosin I HCK activity is enhanced approximately 50 -fold by autophosphorylation. The autophosphorylation of this kinase is enhanced in the presence of acidic phospholipids (Brzeska *et al.*, 1990b). Phosphorylation leads to an increase in the molecular mass of myosin I heavy chain kinase from 97 to 107 kDa (Brzeska *et al.*, 1990b). Presently, the sites of autophosphorylation are unknown.

Distribution of Actin and Myosin

Skeletal Muscle

Skeletal muscle is organized into parallel bundles of muscle fibers. These are giant multinucleated cells that are formed during development by the fusion of numerous precursor cells (Alberts *et al.*, 1989a; Voet and Voet, 1990). Individual muscle fibers are comprised of bundles of 1000 1-2 μm diameter cylindrical myofibrils (Voet and Voet, 1990). Isolated myofibrils possess repeating in-register bands along their length which are responsible for the striated appearance of skeletal muscle. Electron microscopy shows that the myofibrils of resting muscle consist of 2.5-3.0 μm diameter repeating units called sarcomeres. Within each sarcomere, electron dense dark bands, known as **A bands**, alternate in a repeating manner with lighter **I bands**. Each I band is bisected by a narrow **Z disk** (Darnell *et al.*, 1990a).

The A bands consist of a central zone, the AH zone, bordered on both sides by a more electron dense AI zone. In the center of the AH zone is a region known as the M disk or line. The AH zone consists of a bundle of 150 Å diameter thick filaments made up of myosin (Darnell *et al.*, 1990a). Thin filaments of the I band extend from the Z disk and interdigitate with the myosin thick filaments comprising the A band. The I band contains twice as many filaments as the A band (Voet and Voet, 1990). Thick and thin filaments interdigitate where they associate at the electron dense segment of the A band. As discussed later, contraction and relaxation of striated muscle is effected through the relative sliding of thin and thick filaments past each other within the sarcomeres.

Smooth Muscle

The inner lining of the stomach, uterus, intestines, arterial walls, and secretory gland ducts is comprised mainly of *smooth muscle* (Voet and Voet, 1990). This type of muscle is distinct from skeletal muscle tissue in at least three aspects. First, there is a conspicuous absence in smooth muscle of the cross-striations that are characteristic of skeletal muscle. Second, smooth or involuntary muscle is composed of single, mononucleated, spindle-shaped cells which lack the highly organized arrangement seen in skeletal/cardiac muscle. In light of the variety of locations throughout the body where smooth muscle can be found, and the diverse array of contractile processes mediated by smooth muscle, the absence of a fixed arrangement is perhaps not unexpected. Finally, the manner in which smooth muscle regulation is effected differs in several respects from that of skeletal muscle.

There are two basic types of smooth muscle (SM): *multisubunit* and *visceral* smooth muscle (Guyton, 1981a). Multisubunit SM is found in several places in the body, including the ciliary muscle of the eye, and the piloerector muscles which mediate the erection of hairs when stimulated. Visceral SM is located in most of the organs of the body. The major distinction between these two types of SM appears to reside in the manner in which contraction is effected and whether regulation is exerted through nerve signals or by some other stimuli. In multisubunit SM, each smooth muscle fiber is innervated by a single nerve ending and functions independently of the other fibers. Furthermore, control is exerted over individual fibers primarily through nerve signals. In contrast, visceral SM, because of its organization into sheets or bundles, will undergo contraction on a global level when stimulated to do so. Furthermore, control of visceral SM contraction is hormonally regulated at the tissue level (Guyton, 1981a).

Thin and thick filaments are distributed throughout the cytoplasm of smooth muscle cells. Both types of filaments are arranged parallel with the long axis of the the cell. Thin filaments (actin) are complexed with tropomyosin, but lack a troponin component. They are anchored into dense bodies within the cytoplasm. Smooth muscle thick filaments (myosin II) are slightly larger than skeletal muscle thick filaments in both diameter and length (Wolfe, 1993).

Vertebrate Retina

The retina is the light-sensitive region of the vertebrate eye. This multilayered structure is the location of the rod and cone photoreceptors. The cones are responsible for color vision, the rods for vision in the dark (Guyton, 1981b; Darnell *et al.*, 1990b). Photoreceptors are highly polarized cells. Their outermost segment (OS) is connected at one end to the pigment epithelium, and to the rest of the cell via a non-motile cilium consisting of a 9+0 arrangement of microtubules (Alberts *et al.*, 1989b). The outer segment (OS) of rods is composed of several hundred disk membranes stacked upon one another in plate-like fashion. These disks are the location of the photoreceptor pigment, rhodopsin. This integral membrane protein is vectorially transported to the connecting cilium from the inner segment where it is produced and packaged into vesicles (Chaitin *et al.*, 1984).

A number of studies encompassing a variety of techniques have demonstrated the presence of actin and myosin in the outer vertebrate retina. Drenckhahn and Groschel-Stewart (1977) used immunofluorescence microscopy in conjunction with affinity-purified antibodies against chicken gizzard actin and myosin to investigate the presence and distribution of actin and myosin within the ocular cells of frog and rat. These investigators

reported the localization of actin and myosin in rat corneal epithelial cells, anterior lens epithelial cells, rod inner segments, and in frog and rat pigment epithelial cells. Electron microscopy was also used in this study to demonstrate the presence of thin and thick filaments in the size range of 5-8 and 9-11 nm diameter. These sizes correspond to the thickness range reported for actin and myosin filaments, respectively. A correlation between the immunofluorescent labeling and the location of thin filaments was also noted in this study.

Arikawa and Williams (1991), colocalized actin and the actin filament cross-linking protein, alpha-actinin, using immunogold electron microscopy of chicken retina. This study also entailed the use of Phalloidin-FITC for labeling actin filaments. Anti-actin antibodies were localized to the basal microvilli, apical processes of the retinal pigmented epithelium, the plaques of RPE cell-cell adherens junctions, the outer limiting membrane plaques, and the photoreceptor myoids and ellipsoids (Arikawa and Wiiliams, 1991). Alpha actinin was localized to the myoid and to the ellipsoid (Arikawa and Williams, 1991).

This distribution of actin and alpha actinin was reported to be in agreement with other studies, including a report by Chaitin *et al.*, (1984), who used anti-actin antibodies to demonstrate the presence of actin in *Rana pipiens* retina. The anti-actin antibodies labeled the pigment epithelium, pigment epithelium processes, and the distal region of the connecting cilium joining the inner and outer segments of rods and cones (Chaitin *et al.*, 1984). This work is also consistent with a report by Philp and Nachmias (1985), which entailed the immunofluorescent localization of actin, alpha actinin, myosin, and vimentin to chick embryo retinas. Evidence was presented in that report for the distribution of these proteins within the zonula adherens,

apical processes, and in the basal aspect of retinal pigmented epithelial cells. In addition, labeling of actin filaments by Phalloidin has been reported (Philp and Nachmias, 1985; Drenckhan and Wagner, 1985; Vaughan and Fisher, 1987).

A study by Williams *et al.*, (1992) reported the immunogold localization of myosin II heavy chain antibodies to a segment of the connecting cilium, a retinal component previously shown to contain actin filaments (Chaitin, 1984). In addition, these authors presented evidence for myosin ATPase activity in isolated rod outer segments.

The convincing evidence for the presence of actin, myosin II, and several actin-binding proteins in association with the vertebrate retina, supports the general notion that an actomyosin contractile system exists within this system. A number of studies have speculated on the potential function of such a system. Several studies have demonstrated that cytochalasin D interferes with disk membrane morphogenesis (Vaughan and Fisher, 1987; Williams *et al.*, 1988), thus suggesting that actin has a functional role in this process. At the present time, it is unclear as to the specific role played by actin in the mechanism of disk morphogenesis.

Further evidence for the involvement of a contractile apparatus in retinal activity comes from a study of Teleost fish retinas. The retinal cones of fishes contract in the light and elongate in the dark. Burnside (1978) used electron microscopy in conjunction with myosin subfragment-1 binding to study the distribution and polarities of actin and myosin filaments in fish retina, thereby demonstrating a correlation between changes in the distribution and polarity of these two types of filaments with light-induced changes in the shape of cone cells.

Brush Border System of Intestinal Epithelial Cells

The apical region of intestinal epithelial cells is comprised of a complex known as the brush border (BB). This system functions in the resorption of nutrients and electrolytes (Mooseker *et al.*, 1982), a process amplified 15-30-fold by an increased surface area resulting from the presence of microvilli that are 1-2 μm long and 100 nm in diameter (Drenckhahn and Dermietzel, 1988).

The brush border complex consists of two major domains: a region of densely packed hexagonally arrayed microvilli, and the terminal web (Matsudaira and Burgess, 1982). Indirect immunofluorescence (Bretscher and Weber, 1978) and immunoelectron microscopy (Drenckhahn and Dermietzel, 1988) have been used to demonstrate the presence of actin and actin-associated proteins in both the terminal web and the microvilli of brush border cells. In addition, myosin subfragment 1 (S1) decoration has been used to determine the polarity of microfilaments in the microvilli (Mooseker and Tilney, 1975). These investigators showed that all microvillar actin filaments have the same polarity. Myosin subfragment 1 arrowheads all pointed away from the apical tip of the microvilli membrane, toward the terminal web.

The presence of actin within the filamentous network of the microvilli and the terminal web of the BB complex raises the question of whether actin-associated proteins are also localized within this network. Several studies have confirmed the presence in BB of numerous proteins shown to be involved with actin in the contractile process. These include immunogold electron microscopic demonstration of the presence of villin and fimbrin (Drenckhahn and Dermietzel, 1988), and immunofluorescence microscopic

evidence for tropomyosin, filamin, and alpha actinin (Bretscher and Weber, 1978).

In light of the convincing evidence for actin within the BB, several studies have attempted to demonstrate the presence of myosin within this system. Support for myosin II comes from work done by Bretscher (1982), who localized chicken gizzard myosin antibodies to the terminal web region of the BB complex. No labeling of the microvilli was noted in this study. An immunogold electron microscopic study was used to ascertain the qualitative and quantitative distribution of chicken intestinal brush border myosin II (heavy chain), as well as several other actin-associated proteins, in the intestinal BB (Drenckhahn and Dermietzel, 1988). This study confirmed previous reports suggesting that myosin is confined to the terminal web. More specifically, evidence was presented here for myosin II heavy chain in association with the basal half of the terminal web and, to a lesser extent, the apical half (Drenckhahn and Dermietzel, 1988).

Evidence for a nonconventional (single-headed) myosin, now called myosin I, within the BB complex came from studies of a 110 kDa/calmodulin component associated with the microvillus core of avian intestinal brush border. The microvillus core is composed of 15-30 actin filaments arranged in cross-linked bundles (Drenckhahn and Dermietzel, 1988), in addition to five major polypeptides of molecular weight 110, 95, 68, 43, and 17 kDa (Bretscher, 1982). These microfilament bundles are attached to the surrounding plasma membrane through a helical array of lateral linkages. These linkages, called lateral arms, are arranged along the length of the microvilli with a periodicity of 33 nm (Matsudaira and Burgess, 1979). Solubilization of the plasma membrane with Triton X-100 detergent leaves

these linkages intact, while treatment of microvilli with ATP/Mg^{2+} dissociates these cross-bridges from the microfilament bundles of both intact microvilli and isolated demembranated microvilli (Matsudaira and Burgess, 1979). Evidence now exists to support the view that these lateral linkages are comprised, at least in part, of the 110 kDa/calmodulin complex.

Conclusive identification of the 110 kDa/CM complex as a member of the myosin I family of ATPases came from a study by Garcia *et al.*, (1989), who used a lambda gt11 expression library to isolate a cDNA clone encoding 1000 amino acids of the 110 kDa protein. This 3,126-bp clone encodes a protein that has a relative molecular mass of 114,330 D (Garcia *et al.*, 1989).
An array of monoclonal and polyclonal antibodies raised against the 110 kDa protein were immunoreactive with the bacterially-produced fusion protein encoded for by this cDNA (Garcia *et al.*, 1989). Similar to the purified 110 kDa protein, this fusion protein was shown to bind calmodulin (Garcia *et al.*, 1989). These data are in agreement with other binding studies (Glenney and Glenney, 1985) demonstrating maximum binding efficiency in buffers containing Ca^{2+} (Garcia *et al.*, 1989).

The deduced amino acid sequence of this protein showed it to consist of two domains, an amino-terminal > 80 kDa "head" fused to a 35 kDa carboxy-terminal "tail" region (Garcia *et al.*, 1989). The head domain was shown to be homologous to the S1 region of nematode skeletal muscle myosin heavy chain, bovine myosin I, and *Acanthamoeba* myosin IB (Garcia *et al.*, 1989). No homology was found between the tail region of this protein and that of the alpha helical coiled-coil tail of conventional myosin (Garcia *et al.*, 1989). However, a high degree of homology was noted between the carboxy-terminal regions of the chicken BB protein and bovine myosin I.

The homology between the 110 kDa protein and other myosins I is further exemplified by the plasma membrane association of the 110 kDa/CM complex. Similar to all members of the myosin I class whose membrane-binding capacity has been ascertained, the 110 kDa protein has been shown to be plasma membrane-associated. In addition to supportive evidence for 110 kDa/CM being a component of the lateral linkages between the actin bundle and plasma membrane, evidence has been presented identifying 110 kDa as an integral membrane protein (Glenney and Glenney, 1984). These data are consistent with the identification of the 110 kDa/CM protein being a myosin I-like protein (Garcia *et al.*, 1989).

Actin in The Ciliated Protozoan Tetrahymena

Until very recently, the existence of actin in the ciliate *Tetrahymena* has been highly controversial. Research efforts over the past decade have put to rest early speculations on the existence of actin in this organism, and have greatly enhanced our general understanding of protozoan actin.

Metenier (1984) reported that heavy meromyosin localized to basal body-associated filaments in the oral apparatus of *Tetrahymena vorax*. Peck *et al.*, (1991) used immunoblotting to show that an anti-actin monoclonal antibody was immunoreactive with a 43 kDa *Tetrahymena pyriformis* cytoskeletal protein. Studies on purified actin from *Tetrahymena pyriformis* acetone powders showed that on 2-D gels it had a molecular mass of 43.5 kDa and an isoelectric point of 5.4 (Hirono *et al.*, 1989). The primary structure of *Tetrahymena* actin has been deduced from the single-copy, intronless, gene sequence (Cupples and Pearlman, 1986; Hirono *et al.*, 1987a). It is divergent from other actins, having only 75% homology with actins from other organisms (Cupples and Pearlman, 1986; Hirono *et al.*, 1987a). *In vitro*,

Tetrahymena actin polymerized into 6 nm filaments, activated myosin subfragment-1 ATPase (Hirono, 1989), and copolymerized with skeletal muscle actin (Hirono *et al.*, 1990). However, it did not bind DNase 1 or phalloidin (Hirono *et al.*, 1989). An antibody against the predicted N-terminal peptide of *Tetrahymena* actin has been localized to cortical rows of basal bodies, oral apparatus, division furrows, intranuclear filaments, contractile vacuole pores, and food vacuoles in *Tetrahymena* by immunofluorescence microscopy (Hirono *et al.*, 1987a, 1987b).

OBJECTIVES

In light of the profound interest in contractile systems, and the recent convincing identification of actin in the ciliated protozoan *Tetrahymena*, (Hirono *et al.*, 1987a; 1987b; 1989), this study was undertaken with three major objectives in mind: (1) to provide ultrastructural evidence for actin in *Tetrahymena*, (2) to identify and localize myosin-like proteins in *Tetrahymena* and (3) to determine whether myosin ATPase activity exists in *Tetrahymena*.

EXPERIMENTAL DESIGN

The organism used in this study was the ciliated protozoan *Tetrahymena thermophila.* This pear-shaped ciliate is approximately 50 μm in length, and its cortex contains 17-21 longitudinal ciliary rows with associated basal bodies, microtubule bands, and fibrillar elements (Fig. 1). For a recent review of ciliate structure and patterning the reader is referred to Frankel (1989).

The anterior region of this organism contains a feeding complex known as the oral apparatus (OA) which is a composite structure of ciliary units, fibrillar elements, and membranous domains (Fig.2). The OA has been shown by several investigators to be a probable source of *Tetrahymena* actin filaments (Gavin,1976a; Hirono *et al.*, 1987a, 1987b). Moreover, procedures for the isolation of this organelle have long been established and are relatively straightforward. Taking advantage of these characteristics, isolated oral apparatuses from *Tetrahymena thermophila* were used as an immunogen for the production of a polyclonal antiserum containing antibodies against numerous oral apparatus polypeptides. Immunoblotting was used to determine the cross-reactivity of the antiserum with muscle actin and myosin. The reactivity of this antiserum with chicken muscle actin and chicken muscle myosin II light chains was the basis for the affinity purification of antibodies against *Tetrahymena* actin and a putative myosin light chain polypeptide. Immunofluorescence microscopy and immunoelectron microscopy were used to localize these affinity-purified antibodies in *Tetrahymena.* Control experiments utilized preadsorbed antibody for immunoblotting and immunogold electron microscopy.

Quantitative analysis of gold particle distribution was done to ensure the immunospecificity of the antibodies used in this study. To provide further evidence for an actomyosin system, a functional study was undertaken in which a *Tetrahymena* cortical fraction was assayed for ATPase activity using vanadate controls in order to rule out the possibility of contaminating axonemal dynein ATPase activity.

MATERIALS AND METHODS

Cell culture

Tetrahymena thermophila was grown at 35°C in a medium consisting of 2% bacto peptone (Difco) and 0.4% yeast extract (Difco).

Oral apparatus isolation

Isolated oral apparatuses were used as a source of basal body proteins. Procedures for isolation of oral apparatuses from *Tetrahymena thermophila* have been described by Wolfe (1970) and Gavin (1980). A soluble fraction enriched for basal body proteins was obtained by extracting isolated oral apparatuses with 1.0 M KCl as previously described (Gavin, 1977, 1980; Gavin *et al.*, 1989).

Tetrahymena cortical fractions

Cortical fractions which contained cytoskeletons and mucocyst material were isolated from late stationary phase cultures grown at 35°C. Cells were concentrated by centrifugation and washed in a buffer containing 50 mM HEPES (N-2-hydroxyethylpiperazine N-1-ethanesulfonic acid) at pH 6.9, 1 μg/ml leupeptin, and 1 mM PMSF (phenylmethylsulfonyl fluoride). Pelleted cells were resuspended in the HEPES buffer containing 1% Triton-X 100 for 5 minutes at 4°C. The lysate was centrifuged at 10,000 x g for 15 minutes to pellet Triton-insoluble material. The pellet contained cytoskeletons overlaid by a gelatinous layer of mucocyst material. The cytoskeleton-mucocyst material was solubilized for electrophoretic analysis.

Antibodies

Anti-*Tetrahymena* actin antibody: Chicken muscle actin linked to agarose was used to affinity-purify an actin antibody from an antiserum derived by immmunizing a rabbit with a KCl-soluble, oral apparatus fraction enriched for basal body proteins.

Anti-chicken muscle actin antibody: Chicken muscle actin linked to agarose was used to affinity-purify an actin antibody from an antiserum directed against chicken back muscle. This antiserum was purchased from Sigma Chemical Co., St. Louis, Mo.

Monoclonal anti-*Amoeba* actin antibody: This antibody was purchased from Sigma Chemical Co. and used as ascites fluid without further purification.

Anti-myosin light chain-like antibody: Chicken muscle myosin light chains (16, 18, and 25 kDa components; Sigma Chemical Co., St. Louis, MO.) linked to agarose was used to affinity-purify an anti-myosin light chain-like antibody from oral apparatus antiserum.

Immunization

KCl-solubilized, oral apparatus basal body proteins were precipitated by dialysis against distilled water. Approximately 1 mg of the precipitated protein was resuspended in PBS (0.03 M sodium phosphate, pH 7.2, 0.01 M sodium chloride), emulsified with equal volume of Freund's complete adjuvant, and injected into a female, New Zealand rabbit. A second injection of 1 mg of protein in Freund's incomplete adjuvant was given 21 days later and, on day 42, the final injection of 1 mg of protein in Freund's incomplete adjuvant was administered. A test bleed on day 47 confirmed the presence of antibodies against oral apparatus proteins. The rabbit was exsanguinated on

day 54 and the antiserum stored at -20°C. Rabbit boarding, injections, and bleedings were carried out by Pocono Rabbit Farms; Canadensis, PA.

Protein A-purification of antisera

Antisera were dialyzed against 100 mM Tris-HCl, pH 8.0, at 4°C and applied to a column containing 2 ml of protein A-agarose (Bio-Rad; Richmond, CA) that had been equilibrated with 100 mM Tris-HCl, pH 8.0. An antiserum was applied to the affinity column and allowed to bind for 2 h at 4°C. The column was then washed sequentially with 100 mM Tris, pH 8.0, and 10 mM Tris, pH 8.0, until the absorbance at 280 nm was zero. The IgG fraction was eluted from the column with 100 mM glycine at pH 3.0. 1 ml Fractions were collected into tubes containing 50 µl of 1.0 M Tris-HCl, pH 8.0. The eluted fractions were dialyzed against PBS and used for immunodetection experiments.

Affinity-purification of anti-actin antibodies

An affinity resin was prepared by linking chicken muscle actin to activated agarose (affigel-15; Bio-Rad, Richmond, CA) following the directions supplied by the manufacturer. An antiserum was dialyzed overnight against 100 mM Tris-HCl, pH 8.0, applied to a column containing 2 ml of actin-linked affigel-15, and allowed to bind for 2 h at 4°C. The column was then washed with TBS until the absorbance at 280 nm was zero. Anti-actin antibodies were eluted with 100 mM triethylamine at pH 11.5. 1 ml Fractions were collected and treated as described above.

Affinity-purification of anti-myosin light chain-like antibodies (anti-18 kDa)

An affinity resin was prepared by linking chicken muscle myosin light chains (Sigma Chemical Co.) to activated agarose (affigel-15; Bio-Rad, Richmond, CA) following the directions supplied by the manufacturer. An antiserum against oral apparatus basal body proteins was dialyzed overnight against 100 mM Tris-HCl, pH 8.0, applied to a column containing 2 ml of myosin light chain-linked affigel-15. and allowed to bind for 2 h at 4°C. The column was then washed with TBS until the absorbance at 280 nm was zero. Anti-myosin light chain-like antibodies were eluted with 100 mM triethylamine at pH 11.5. 1 ml Fractions were collected and treated as described above.

Immunoadsorption

Affinity-purified anti-*Tetrahymena* actin antibody was diluted 1:2 with 1% chicken muscle actin (Sigma Chemical Co.) in PBS. The mixture was incubated at room temperature for 2 h and then used for immunodetection of antigens on nitrocellulose membranes and on sectioned material in conjunction with colloidal gold.

Immunofluorescence

Log phase cultures of *Tetrahymena thermophila* were concentrated and resuspended in 100 mM Tris, 10 mM EDTA, pH 8.0. The cells were chilled at 4°C for 5 min, then permeabilized and fixed in 35% ethanol containing 0.5% Triton X-100 for 5 min. The fixed cells were washed in PBS containing 3% Fraction V BSA (Sigma Chemical Co.) and resuspended in fresh PBS/BSA for

30 min. Washed cells were incubated for 1 h with affinity-purified anti-*Tetrahymena* actin antibody diluted 1:10 with the PBS/BSA solution. Cells were then washed with PBS and incubated for 45 min in fluorescein-labeled secondary antibody diluted 1:100 with PBS/BSA. The labeled cells were washed extensively with PBS and viewed with an Olympus fluorescence microscope. Images were recorded on Kodak Technical Pan film.

Electron microscopy

Isolated oral apparatuses and log phase *Tetrahymena* cells were fixed in 1% glutaraldehyde in 0.1 M sodium cacodylate, pH 7.2, for 1 h at 4°C. After centrifugation, the pellets were washed with buffer and incubated for 1 h in 2% Osmium Tetroxide in cacodylate buffer, followed by dehydration by sequential washings in 50% and 70% ethanol at 4°C. The pellets were then infiltrated for 30 min in a 2:1 mixture of LR White (Polysciences; Warrington, PA): 70% ethanol, followed by pure LR White for 1 h, all at 4°C. The pellets were infiltrated with fresh resin overnight at 25°C and, following centrifugation and resuspension in fresh resin, cured in Beem capsules for 24 h at 60°C. Thin sections were cut with a diamond knife and collected on 300 mesh Square Thinline grids (Polysciences; Warrington, PA.).

Immunogold labeling

Sections on grids were floated on 60 μl droplets of a 10% solution of heat-inactivated normal goat serum (Zymed; San Francisco, CA) in 0.1 BSA in PBS buffer for 20 min, washed extensively in PBS buffer, and incubated in primary antibody diluted in 0.1% BSA in PBS. The sections were incubated for 2-24 h in a 1: 2 dilution of affinity-purified anti-actin antibody, followed

by extensive washing with PBS and incubation for 2 h on 25 μl droplets of anti-IgG secondary antibody linked to 15 nm colloidal gold particles (Sera-lab; Westbury, NY) diluted either 1:20 or 1:30 in 0.1% BSA in PBS. Following incubation in secondary antibody, sections were washed sequentially in PBS and distilled water, stained with uranyl acetate (aqueous) and lead citrate (Reynold's), and observed with a Philips EM 300 electron microscope. For controls, primary antibody was omitted, and the sections were treated in the same manner as sections incubated in primary antibody.

Double labeling

Sections were floated on 60 μl droplets of a 10% solution of heat-inactivated normal goat serum (Zymed; San Francisco, CA) in 0.1% BSA in PBS buffer for 20 min, washed extensively in PBS buffer, and incubated for 24-40 h in affinity purified anti actin antibody diluted 1:2 in 0.1% BSA in PBS. The sections were washed extensively with PBS, followed by incubation for 2 h on 25 μl droplets of anti-IgG secondary antibody linked to 15 nm colloidal gold particles (Sera-lab; Westbury, NY) diluted either 1:20 or 1:30 in 0.1% BSA in PBS. The sections were then washed extensively with PBS and distilled water. The sections were incubated for 24 h in affinity purified anti-17 kDa antibody diluted 1:3 in 0.1% BSA in PBS, washed extensively in PBS buffer, followed by incubation in secondary antibody linked to 5 nm colloidal gold particles (Sera-lab; Westbury, NY). Sections were then washed sequentially in PBS buffer and distilled water, followed by staining with aqueous uranyl acetate and Reynold's lead citrate prior to being observed with a Philips EM 300 electron microscope.

Morphometric analysis

A morphometric analysis employed stereological principles described by Weibel *et al.*, (1966). Three different colloidal gold labeling experiments were treated as separate samples. Electron micrographs from each sample were analysed by using a transparent sheet marked with a squared point lattice consisting of a series of intersecting parallel lines (d=1 mm). The point lattice was placed at random over randomly chosen micrographs of immunogold labeled sections. Points lying on colloidal gold particles over organelles were scored according to component type (i.e., cage walls). Relative colloidal gold particle density over each organelle was computed for each sample as described by Weibel *et al.*, (1966).

Electrophoresis and immunoblotting

Oral aparatus proteins were solubilized at 37°C in Laemmli (1970) sample buffer containing 5% ß-mercaptoethanol. Proteins were separated on 12% SDS-polyacrylamide gels (Laemmli, 1970) and electrophoretically transferred to nitrocellulose membranes using the procedure described by Towbin *et al.*, (1979). For immunodetection of antigens, nitrocellulose membranes containing transferred proteins were blocked by incubation in 5% non-fat dry milk (Alba) in PBS for 2 h. After two washes in TPBS (PBS with 0.2% TWEEN), membranes were incubated in primary antibody diluted in 3% BSA in PBS. Membranes were incubated for 2 h in a 1:40 dilution of anti-oral apparatus antiserum or in a 1:10 dilution of affinity-purified anti-actin antibody. For control experiments, preimmune serum was used instead of primary antibody. After three washes in TPBS, immune complexes were

detected by incubating the membranes for 1-2 h in a 1:2000 dilution of alkaline phosphatase-conjugated secondary antibody (Bio-Rad; Richmond, CA) in 3% BSA in TBS followed by color development using BCIP and NBT (Bio-Rad; Richmond, CA) as substrates.

Cytochalasin experiments

Concentrated stock solutions of cytochalasin D were made in dimethylsulfoxide (DMSO). Aliquots of the appropriate stock were added to isolated oral apparatuses in 100 mM Tris, pH 8.0, to give a final concentration of 0.5 mM. Oral apparatuses were incubated in the cytochalasin solution for 20 min at 25°C. After the cytochalasin treatment, the oral apparatuses were centrifuged through two changes of the Tris buffer and fixed for electron microscopy. For controls, oral apparatuses were treated with appropriate concentrations of DMSO and fixed for electron microscopy.

ATPase Assay

ATPase assays were carried out in a volume of 0.5 ml containing appropriate dilutions of oral apparatus fractions and a buffer for either Mg^{+2} or K^{+}-activated ATPase activity. For Mg^{+2}-activated ATPase activity, the buffer contained 2 mM ATP, 2 mM $MgCl_2$, 1mM EGTA, 15 mM imidazole at pH 7.2. For K^{+}-activated ATPase activity, the buffer contained 2 mM ATP, 500 mM KCl, 2 mM EDTA, 15 mM imidazole at pH 7.2. Some assays were carried out in the presence of 10 mM vanadate (Gibbons *et al., 1978*). Activity was measured after 5 minutes incubation at 35°C by stopping the reaction with cold TCA and assaying for total phosphate.

Amino acid composition analysis

Oral apparatus proteins were separated by SDS-PAGE and transferred to a polyvinylidene difluoride membrane (Bio-Rad). One lane of proteins was stained with Coomassie Blue and used as a marker for the identification of bands which were excised from the unstained membrane. The membrane containing excised protein was washed several times in deionized water. Amino acid composition analysis was performed from acid hydrolysates of the membrane-bound protein by the Woods Hole Protein and Nucleic Acid Center.

RESULTS

Antibodies

Oral apparatus antiserum

An anti-oral apparatus antiserum was prepared by immunizing a rabbit with a KCl-soluble oral apparatus fraction that was enriched for basal body proteins. The specificity of this antiserum for oral apparatus polypeptides was determined by immunoblotting. Total oral apparatus proteins (fig. 3b) were transferred to a nitrocellulose membrane and probed with the anti-oral apparatus antiserum (fig. 3c). The antiserum was immunoreactive with many oral apparatus polypeptides including a putative *Tetrahymena* actin, a 44 kDa polypeptide (fig. 3c, arrowhead). Preimmune serum was not immunoreactive with oral apparatus polypeptides (fig. 3d).

The oral apparatus antiserum was tested for cross-reactivity with chicken muscle actin and chicken muscle myosin light chains on immunoblots. The antiserum was immunoreactive with chicken muscle actin (fig. 4c) and the 25 kDa and 18 kDa myosin light chains (fig. 5c).

Anti-actin antibodies

The affinity of the anti-oral apparatus antiserum for chicken muscle actin was the basis for the affinity purification of a subset of antibodies specific for actin (see Materials and Methods). Total apparatus proteins (fig. 6b) or cortical fraction proteins were transferred to a nitrocellulose membrane and probed with the affinity-purified anti-*Tetrahymena* actin antibody (fig. 6c). The affinity-purified antibody was immunospecific for a 44 kDa *Tetrahymena* oral apparatus polypeptide (fig. 6c). The affinity-

purified anti-*Tetrahymena* actin antibody cross-reacted with muscle actin on immunoblots (fig. 4d).

To further show that the affinity-purified antibody was specific for an actin epitope, the antibody was preadsorbed with muscle actin. The preadsorbed antibody did not bind to oral apparatus proteins on immunoblots (fig. 6e).

Chicken muscle actin linked to agarose was used to affinity-purify anti-chicken muscle actin antibody from an anti-chicken muscle actin antiserum. The affinity-purified, anti-chicken muscle actin antibody cross-reacted with *Tetrahymena* actin on immunoblots (fig. 6d).

Anti-18 kDa antibodies

The cross-reactivity of the oral apparatus antiserum with muscle myosin light chains (MLC) was the basis for the affinity purification of a subset of antibodies specific for an 18 kDa *Tetrahymena* polypeptide. Total apparatus proteins (fig. 7b) were transferred to a nitrocellulose membrane and probed with the affinity-purified anti-*Tetrahymena* MLC-like antibody. The affinity-purified antibody was monospecific for an 18 kDa oral apparatus polypeptide (fig. 7c). The affinity-purified antibody did not cross-react with muscle actin on immunoblots.

Immunofluorescence Localization of Anti-Actin Antibodies

Immunofluorescence microscopy was used to localize the affinity-purified anti-*Tetrahymena* actin antibody in *Tetrahymena.* The antibody localized to longitudinal cortical rows which contain basal bodies and mucocysts, and to the oral apparatus, which is the bright curved band at the anterior of each cell (fig. 8a). Preimmune serum did not label any structures

in *Tetrahymena* cells (fig. 8b).

Immunogold Localization of Anti-Actin Antibodies

In order to map the ultrastructural location of anti-actin binding sites within *Tetrahymena,* affinity purified anti-actin antibodies were used in conjunction with immunogold labeling of LR White-embedded *Tetrahymena* cells. At electron microscopic resolution, the affinity-purified anti-*Tetrahymena* actin antibody localized to basal body-associated fibrillar structures, mucocysts, cytoplasmic filaments, and the macronucleus in *Tetrahymena.* These labeling patterns are documented in a series of electron micrographs (figs. 9-15).

Localization to basal body-associated fibrillar structures

The affinity-purified anti-actin antibody localized to both somatic and oral basal bodies in *Tetrahymena* cells. Somatic basal bodies are arranged in longitudinal rows in which a basal body alternates with a mucocyst. Sections which contained *in situ* somatic basal bodies were stained with affinity purified anti-*Tetrahymena* actin antibody followed by secondary antibody linked to 15 nm colloidal gold particles. Fig. 9 shows two basal bodies and two empty mucocyst sites. One of the basal bodies is not completely in the plane of section. Colloidal gold particles decorated the basal body wall, basal plate region, and filaments (arrow) at the proximal end of the basal body (fig. 9).

In order to further characterize the labeling of basal body-associated structures by the anti-actin antibody, the antibody labeling of isolated oral apparatuses was investigated. The *Tetrahymena* oral apparatus contains a heterogeneous network of filaments (Gavin, 1980; Williams, 1986). A cylindrical, filamentous cage (Williams, 1986) surrounds each basal body

(Fig. 10) For convenience, the basal body-cage complex can be divided into four regions (Fig. 10):

Basal Body Walls. The basal body walls consist of the microtubule boundaries of the entire cylinder except the basal plate.

Basal Plate. The basal plate is characterized in transverse section by a rosette of fibers around basal body microtubules, and in longitudinal section by dense transverse fibers at the end of the cylinder closer to the cell surface. The basal plate forms the top of the basal body cage.

Proximal Filaments. In longitudinal section, the end of the basal body cylinder farther from the cell surface contains interwoven filaments which form the base of the basal body cage.

Cage Wall Filaments. The cage wall around oral basal bodies consists of a cylindrical filamentous partition connected to the basal body wall by a network of filaments. The cage wall associated with somatic basal bodies consists of the postciliary fiber and the kinetodesmal fiber.

Figure 11a shows a row of basal bodies in the isolated oral apparatus and the close association between basal body microtubules and basal body cage filaments. Figure 11b is a longitudinal section of basal bodies in a membranellar row in an isolated oral apparatus. The distal end of each basal body contains a short segment of ciliary axoneme. During the isolation of oral apparatuses, axonemes become detached at a point near the basal plate (Fig. 11a). Although each basal body is enclosed by a filamentous cage, the walls (arrowheads) of a single cage are in the plane of section in figure 11a. In figure 11b, the plane of section is through a region where basal body microtubules (arrows) are connected to cage walls (arrowheads) by a network of thin filaments, some of which are 5-6 nm in diameter. The cloud of filaments at the top of the micrograph appear to be continuous with the

walls of the basal body cages. The dense network of fibers at the proximal region form the base of the cage from which emanate accessory microtubules (Fig. 11b).

The affinity-purified anti-*Tetrahymena* actin antibody specifically labeled actin epitopes in four distinct regions of the basal body cage complex: (a) basal body walls, (b) basal plate filaments, (c) filaments at the proximal end, and (d) cage wall filaments. In addition, the antibody labeled filament bundles that interconnect groups of basal bodies (membranelles) within the oral apparatus. These labeling patterns are documented in a series of electron micrographs (figs. 12-14).

Fig. 12 is a transverse section through an isolated oral apparatus labeled with affinity-purified anti-*Tetrahymena* actin antibody followed by IgG secondary antibody linked to 15 nm colloidal gold particles. Colloidal gold particles were closely associated with basal body microtubules. Fig. 13 shows a longitudinal view of basal bodies in an isolated oral apparatus stained with affinity-purified, anti-*Tetrahymena* actin antibody. Colloidal gold decorated the entire length of the basal body from its proximal terminus to the basal plate (fig. 13a). The dense layer of interwoven filaments (fig. 13a) at the proximal end of each basal body form the base of the basal body cage. These filaments are labeled with colloidal gold. Labeling of the cage wall is shown in a longitudinal section through basal bodies in an isolated oral apparatus stained with affinity-purified, anti-*Tetrahymena* actin antibody followed by secondary antibody linked to 15 nm colloidal gold particles (fig. 13b). Although basal bodies are not in the plane of section, cage walls are visible and labeled with colloidal gold (fig. 13b). Labeling of the cage wall is also shown in transverse sections through isolated oral apparatuses stained with anti-*Tetrahymena* actin antibody followed by secondary antibody linked to

15 nm colloidal gold (fig. 14). In this figure, colloidal gold particles are closely associated with regions of the basal body wall where filaments project (thin arrows, fig. 14). These filaments connect the basal body wall with the cage wall (bold arrow, fig. 14). The rosettes around basal bodies are formed from interwoven filaments of the basal plate which form the top of the cage (fig. 14). The right margin of the micrograph in fig. 14 shows labeling of basal plate filaments. The long filament bundles connecting one row of basal bodies with another row are also immunoreactive with the antibody (fig. 14).

Controls for immunospecificity

Several controls were done to ensure the specificity of the localization to basal body-associated fibrillar components. When sectioned material was incubated in preimmune serum instead of primary antibody, or incubated with secondary antibody without prior incubation in primary antibody, only randomly distributed gold particles were observed. When the anti-*Tetrahymena* actin antibody was preadsorbed with chicken muscle actin and used to label sections of isolated oral apparatuses, only randomly dispersed colloidal gold particles were observed (fig. 15). To further demonstrate that basal bodies and their associated filaments contain specific antigenic sites immunoreactive with anti-actin antibodies, affinity purified anti-chicken muscle actin antibody was used with the immunolabeling technique. This antibody labeled the same regions of the basal body-cage complex as the anti-Tetrahymena actin antibody (data not shown). Moreover, a monoclonal antibody against an *Amoeba* actin epitope labeled the same regions of the basal body-cage complex as the two polyclonal antibodies (data not shown).

Localization to in situ mucocysts

Mucocysts are protozoan secretory organelles containing a highly condensed, crystalline material (Hausman, 1978; Tokuyasu and Scherbaum, 1965). In *Tetrahymena,* they are docked at the cell surface between and within the ciliary rows (Allen, 1967). Although the precise function of these organelles remains enigmatic, possible functions include protection for the cell through the secretion of a gelatinous coat (Hausman, 1978), and extracellular digestion (Tiedtke and Gortz, 1983).

The affinity-purified, anti-actin antibody was used in conjunction with the immunogold labeling technique to localize the antibody to *Tetrahymena* mucocysts. Thin sections were labeled with the antibody followed by secondary antibody linked to 15 nm colloidal gold particles. Fig. 16 shows a section through the cortical region of a *Tetrahymena* cell. Several spindle-shaped mucocysts were docked at the cell surface (arrowheads, fig. 16). Colloidal gold particles were located throughout the mucocyst matrix in these mucocysts (fig. 16). A grazing section through a docked mucocyst revealed immunoreactive thin filaments closely associated with mucocyst material (fig. 17a). Some of these filaments were most clearly observed at the periphery of the mucocyst material (arrowhead, fig. 17a). The mucocyst membrane was not distinct in some preparations embedded in LR White resin.

For control experiments, sections through the *Tetrahymena* cortex were treated with preimmune serum followed by secondary antibody linked to 15 nm colloidal gold particles. Only a few particles random gold particles were observed in sections treated with preimmune serum (fig. 18).

Localization to discharged mucocyst material

During the exocytotic process, discharged mucocyst material can partially cover the cell surface (Tokuyasu and Scherbaum 1965). In the present study, a dense filamentous material was lodged on the cell surface near exocytotic sites. This material is presumed to be discharged mucocyst material. These sites were identified by the presence of discharged mucocysts in the adjacent cytoplasm and, in many instances, by the presence of another condensed mucocyst at the cell surface. The fusion pore at these sites had closed, and the integrity of the membrane had been restored. The labeling of the material at these sites by the anti-actin antibody was investigated, and the extent to which discharged mucocysts were labeled by the anti-actin antibody determined.

Fig. 17b shows a section through the cortical region of a cell fixed after discharge of a mucocyst and after closure of the fusion pore. A discharged mucocyst from a previous exocytotic event was evident in the cytoplasm (dm, Fig. 17b). Another condensed mucocyst had moved into the docking site (m, Fig. 17b). Although they were not completely in the plane of focus, a few colloidal gold particles decorated the midregion of the condensed mucocyst (Fig. 17b). A dense material, heavily labeled with colloidal gold particles and presumed to be discharged mucocyst material, was lodged on the cell surface near the exocytotic site and adjacent to two cilia (arrowheads, Fig. 17b). Some of this dense material was lodged in the region where the fusion pore had been located (small arrowheads, Fig. 17b). All of the dense material was enmeshed by a mass of filaments which appeared to be the site of labeling by the anti-actin antibody (arrowheads, Fig. 17b). In contrast to the dense material at the cell surface, the discharged mucocyst adjacent to the exocytotic site showed virtually no labeling by the anti-actin antibody (dm,

Fig. 17b).

Localization to the macronucleus

Nuclear dualism is a ciliate hallmark. All ciliates possess both a micronucleus and a macronucleus. The micronucleus is diploid, and divides either mitotically (in vegetative cells) or meiotically (during sexual reproduction). On the other hand, the macronucleus is polygenic, possessing up to several hundred times the DNA content of the micronucleus (Doerder and Debault, 1975; Blackburn and Karrer, 1986). It divides amitotically in vegetative cells but is degraded during conjugation or autogamy. A new macronucleus differentiates during conjugation from the mitotic division of germ-line micronuclei (reviewed by Blackburn and Karrer, 1986). During macronuclear differentiation, a dramatic reorganization of the genome takes place. This process apparently involves the elimination of micronuclear DNA sequences from the newly forming macronucleus (Blackburn and Karrer, 1986).

The macronucleus in *Tetrahymena* is comprised of several thousand, randomly distributed, spherical, 0.1-0.2 μm diameter chromatin bodies (Pitelka, 1963; Wolfe, 1980). These chromatin bodies are interconnected by a complex array of fibrils (Wolfe, 1967). The general organization of the macronucleus in *Tetrahymena* and its spatial relationship to cortical organelles are shown in fig. 19. The affinity-purified, anti-*Tetrahymena* actin antibody was used in conjunction with 15 nm colloidal gold -labeled secondary antibody to localize actin to fibrillar components of the macronucleus (fig. 20). In this cross-section through a portion of the macronucleus, the antibody labeled filaments (arrows, fig. 20) located

between the dense chromatin bodies (arrowheads, fig. 20).

Quantitative Analysis of Gold Particle Distribution

In order to quantitate the density of colloidal gold particles associated with basal body fibrillar elements, mucocysts, cytoplasmic filaments, and the macronucleus in *Tetrahymena* a morphometric analysis using stereological principles described by Weibel *et al.*, (1966) was performed. Data analysis was achieved by placing a transparent sheet containing a point lattice directly over random electron micrographs. Lattice points coincident with colloidal gold particles over basal body-cage components, docked mucocysts, cytoplasmic filaments, macronuclei, discharged mucocysts, plasma membrane and mitochondria were separately compiled. Relative particle density over each region was computed as described by Weibel *et al.*, (1966). The results of this analysis are shown in Table 1.

In order to determine the extent of particle enrichment over basal body-cage components, docked mucocysts, discharged mucocysts, cytoplasmic filaments and macronuclei, the relative particle density ($\pm$ S.D.) for each of these five regions was compared with the relative particle density over mitochondria which was used a measure of non-specific binding of the antibody (table 1). These comparisons showed that relative particle densities over basal body-cage components and docked mucocysts were respectively enriched at least 12.3 and 8.4 times the relative particle density over mitochondria (table 1). Relative particle densities over cytoplasmic filaments and macronuclei were respectively at least 3.2 and 2.1 times the relative particle density over mitochondria (table 1). The relative particle density over discharged mucocysts showed no enrichment when compared with the relative particle density over mitochondria (table 1).

Immunogold Localization of Anti-18 kDa Antibodies

In order to map the ultrastructural location of the 18 kDa polypeptide, immunogold electron microscopy was used in conjunction with affinity purified anti-18 kDa antibody. Fig. 21 is a longitudinal section through a row of basal bodies in an isolated oral apparatus. In this section, colloidal gold particles were closely associated with basal body microtubules.

Colocalization of Anti-Actin and Anti-18 kDa Antibodies

Double-labeling immunoelectron microscopy was used in order to ascertain the spatial relationship between the epitopes recognized by the anti-actin and anti-17 kDa antibodies. Figure 22 shows a longitudinal section through a row of basal bodies in an isolated oral apparatus. This section was labeled with affinity purified anti-*Tetrahymena* actin and 15 nm colloidal gold anti-IgG (arrow) followed by affinity purified anti-18 kDa and 5 nm colloidal gold anti-IgG (arrowhead). With both antibodies, colloidal gold particles were closely associated with basal body microtubules and fibrillar components of the basal body cage.

Figure 23 is a cross-section through basal bodies in an isolated oral apparatus. This section was labeled with affinity-purified anti *Tetrahymena* actin and 15 nm colloidal gold anti-IgG (arrow) followed by affinity purified anti-18 kDa and 5 nm colloidal gold anti-IgG (arrowhead). This micrograph shows the close association of colloidal gold particles with basal body microtubules.

Control for Double Labeling Immunoelectron Microscopy

The double labeling experiments used two different primary antibodies (IgG) that were produced in rabbits. After application of the first primary

antibody and its secondary antibody, some first primary antibody sites could remain unreacted and could subsequently react with secondary antibody (anti-IgG). In order to demonstrate that the first primary antibody did not have a significant number of unreactive sites after the application of the first secondary antibody, sections were incubated with anti 18 kDa followed by secondary antibody linked to 15 nm colloidal gold particles. The sections were subsequently incubated with unlabeled anti-IgG followed by IgG linked to 5nm colloidal gold particles. The sections were analyzed for the distribution of both 15 nm and 5 nm colloidal gold particles (Table 2, figs., 24 and 25). These data show that the density of 15 nm particles was more than 34 times the density of 5 nm particles. These results indicate that in the double labeling protocol, the first primary antibody did not have a significant number of unreactive sites after the application of the first secondary antibody.

ATPase Assay

Isolated oral apparatuses exhibited Mg^{+2}-EGTA ATPase activity. At pH 7.2,, the ATPase activity was 1.21 ± 0.37 μmole Pi mg^{-1} min^{-1}. Between 60% and 80% of the Mg^{+2}-EGTA activity was insensitive to 10 mM vanadate.

Amino Acid Composition of 18 kDa

An anti-oral apparatus antiserum was immunoreactive with the 25 kDa and the 18 kDa chicken skeletal muscle myosin light chains. These muscle light chains were used to affinity-purify an antibody that detected an 18 kDa *Tetrahymena* polypeptide on immunoblots. The amino acid composition of the 18 kDa polypeptide was determined and compared with published (Weeds and Lowey, 1971) amino acid compositions of the 25 kDa and the 18 kDa

myosin light chains. The mole percent of each amino acid has been expressed as the number of amino acid residues and is shown in table 3. The molecular mass of this polypeptide, based on the number of amino acid residues, is 17, 223 D. The boxed areas show apparent relatedness between the 18 kDa polypeptide and the two muscle light chains with respect to acidic, basic, hydrophilic and hydrophobic amino acids.

DISCUSSION

Specificity of Antibodies Used in This Study

Anti-actin antibody

In this study, an anti-actin antibody was affinity-purified from an antiserum raised against *Tetrahymena* oral apparatus basal body proteins. The antibody was immunoreactive with chicken muscle actin on immunoblots and monospecific for *Tetrahymena* actin on immunoblots containing total oral apparatus protein or cortical fraction proteins enriched for mucocyst material. The specificity of the antibody for actin epitopes was confirmed by preadsorption of the antibody with chicken muscle actin which completely eliminated the binding of the antibody to oral apparatus proteins on immunoblots and to basal body structures with the immunogold labeling technique. It is unlikely that the adsorption effect of the muscle actin was due to contaminating proteins present in the muscle actin preparation, because immunoblotting showed that in this preparation, even under conditions of overloading, the affinity-purified antibody detected only muscle actin (Fig. 4d).

An affinity-purified antibody against chicken muscle actin was also used in this study. This antibody was monospecific for *Tetrahymena* actin on immunoblots containing total oral apparatus protein.

Anti-18 kDa

Agarose-linked chicken muscle myosin light chains were used to affinity-purify an anti-18 kDa antibody from the anti-oral apparatus antiserum. Immunoblot analysis indicated that on immunoblots the antibody

was immunoreactive with chicken muscle myosin 25 kDa and 18 kDa light chain polypeptides, and monospecific for an 18 kDa *Tetrahymena* oral apparatus polypeptide.

18 kDa--a Putative Myosin Light Chain-Like Polypeptide

An affinity-purified antibody cross-reacted with the 25 kDa and the 18 kDa muscle myosin light chains and a *Tetrahymena* polypeptide which was shown by amino acid composition analysis to have a molecular mass of 17, 223 daltons. This cross-reactivity suggests that the *Tetrahymena* polypeptide contains an epitope(s) in common with the two myosin light chains. Although the 25 kDa and the 18 kDa are not chemically related in vertebrate skeletal muscle (Weeds and Lowey, 1971), the cross-reactivity described above suggests a chemical relationship between the 18/17 kDa *Tetrahymena* polypeptide and the two myosin light chains. The probable chemical relatedness between the polypeptides is further suggested by their amino acid compositions. Although the 18/17 kDa *Tetrahymena* polypeptide is clearly different in composition from either the 25 kDa or the 18 kDa chicken skeletal muscle myosin light chains, it has apparent homology with these two myosin light chains with respect to some acidic (glutamic acid), basic (lysine), hydrophilic (threonine, valine, and isoleucine), and hydrophobic (tyrosine and histidine) amino acids (table 3). On the basis of the immunologic and amino acid composition analyses, it is tentatively concluded that the 18/17 kDa is a putative *Tetrahymena* myosin light chain -like polypeptide. Further chemical studies will be required to demonstrate whether 18/17 kDa is a myosin light chain.

Actin and 18/17 kDa Are Components of the *Tetrahymena* Basal Body-Cage Complex

Indirect immunofluorescence was used to show that the affinity-purified, anti-*Tetrahymena* actin antibody localized to both oral and somatic basal bodies. The results with immunofluorescence microscopy are in agreement with the results reported by Hirono *et al.*, (1987b) who used an antibody directed against the predicted N-terminal region of *Tetrahymena* actin.

In order to map the location of actin within the basal body-cage complex, the immunogold labeling technique was used in conjunction with thin sections of LR White-embedded isolated oral apparatuses and LR White-embedded *Tetrahymena* cells. Thin sections were stained with affinity-purified, anti-*Tetrahymena* actin antibody. Morphometric analysis of gold particle density confirmed the specificity of the anti-actin antibody for actin epitopes in four distinct regions of the basal body-cage complex: (a) basal body walls, (b) basal plate filaments, (c) proximal filaments, and (d) cage wall filaments. The analysis also demonstrated that non-specific binding of the anti-actin antibody was negligible and that preadsorption of the antibody with chicken muscle actin effectively eliminated the binding of the antibody to basal body structures.

Double-label immunogold electron microscopy with anti-actin and anti-18/17 kDa antibodies was used to demonstrate the coexistence of actin epitopes and epitopes of the putative myosin light chain-like component within the basal body cage complex. These two affinity purified antibodies colocalized to the basal body walls, basal plate filaments, proximal filaments, and cage wall filaments within the basal body-cage complex.

I have considered the possibility that actin and the putative myosin light chain-like polypeptide associated with the basal body-cage complex were derived from cytosol proteins redistributed during oral apparatus isolation or during preparation of cells for antibody labeling. This is most unlikely because identical labeling patterns were observed using thin sections of isolated oral apparatuses and thin sections of oral apparatuses *in situ*. Furthermore, both immunofluorescence microscopy and immunogold microscopy localized the anti-actin antibody to basal bodies *in situ*. These techniques utilized very different fixation conditions. For immunofluorescence microscopy, cells were permeabilized and fixed in triton-ethanol, whereas for immunogold electron microscopy, cells were fixed in glutaraldehyde without triton permeabilization, and sections of embedded cells labeled directly with the antibody.

Based on the antibody localization studies, it is concluded that actin and the 18/17 kDa putative myosin light chain-like polypeptide are components of basal plate filaments, proximal filaments, and basal body cage filaments, and that these filaments are closely associated with basal body microtubules. These results raise the possibility of an actomyosin contractile system associated with basal bodies.

Actin-microtubule interactions in basal bodies

The micrographs presented in this study show a very clear and obvious close association of colloidal gold particles with basal body microtubules. There are three possible explanations for this labeling pattern:

Basal bodies are enclosed by separate, cylindrical cages which are filamentous structures capped at the top by the basal plate and at the base by interwoven filaments. The cage walls are filamentous partitions connected

to basal body microtubules by a network of thin filaments. The anti actin antibodies could bind to actin filaments from basal body cages at sites where the filaments insert into the basal body wall. This interpretation is consistent with the pattern of colloidal gold labeling in which gold particles were closely associated with basal body microtubules. A study by Williams (1986) provides evidence for a non-actin component of basal body cages. This author reported the localization of an 87 kDa polypeptide to basal body cage filaments. In light of the present study, it seems probable that the basal body cage is a complex of several filament types.

Another interpretation of the labeling of the basal body wall by anti actin antibodies is that the antibodies bind to actin filaments that are not associated with basal body cages. The anti actin antibodies might bind to the filaments located between triplet microtubules. Inter-triplet filaments have been described in basal bodies from several organisms (Gibbons and Grimstone, 1960; Gibbons, 1961; Wolfe, 1970; Gavin, 1977). These filament links repeat along each triplet microtubule. Their function remains unresolved and, to my knowledge, their biochemical composition has never been reported.

Finally, the possibility must also be considered that the anti actin antibodies bind to both G-actin and F-actin in basal bodies. If G-actin were incorporated in the basal body wall, it could bind anti-actin antibodies. G-actin in this location could nucleate the assembly of basal body-associated filaments, e.g., cage filaments.

These three interpretations of the labeling pattern with anti actin antibodies are not mutually exclusive, and the data presented in this work are consistent with all three of them.

Cytochalasin-treated oral apparatuses

The basal body-cage complex is part of a heterogeneous network of filaments within the oral apparatus (Gavin, 1977; Williams, 1986). In the present study, anti actin antibodies labeled basal body-cage filaments and other basal body-associated filaments in the oral apparatus. Although cytochalasin has been shown to bind to isolated oral apparatuses (Gavin, 1976b), prevent oral apparatus development (Gavin, 1976a), and sever actin filaments (Hartwig and Stossel, 1979; Schliwa, 1982), no changes in either the structure of the filament network or its immunoreactivity with anti actin antibodies in cytochalasin-treated oral apparatuses were detected. However, the majority of oral filaments are bundled into large cables and disruption of actin filaments within the cables might not be detected by electron microscopy. If the drug severed actin filaments in the basal body cage, the non-actin filaments of the cage were apparently sufficient to maintain cage integrity. Furthermore, if cage actin filaments were severed by cytochalasin, it seems likely that portions of the filaments would have remained attached to the basal body wall and accessible to anti actin antibodies. The concentration of cytochalasin (0.5 mM) used in the present study is higher than the concentration of the drug usually employed with studies on mammalian cells, but it is comparable to the concentration of the drug used to study actin in *Chlamydomonas* (Detmers *et al.*, 1983; Dentler and Adams, 1992).

Possible functions for the basal body cage

The direct association of actin and a putative myosin light chain-like polypeptide with basal bodies raises the possibility of an actin-based contractile system. The demonstration of vanadate-insensitive ATPase

activity associated with oral apparatuses is further indication that a myosin motor is associated with this putative contractile system. A contractile system associated with basal bodies could cause changes in the orientation of basal bodies during ciliary motion and thereby influence the direction of ciliary wave motion. Alternatively, such a contractile system could prevent changes in the orientation of basal bodies that might otherwise be induced during sliding of axonemal microtubules.

Basal body-associated actin filaments might play a role in orienting basal bodies during new oral apparatus formation. The oral apparatus is formed from an aggregate of basal bodies which migrate into the characteristic membranellar pattern of the oral apparatus. Cytochalasin, an inhibitor of actin filament assembly, prevents this migration of basal bodies and prevents oral apparatus morphogenesis (Gavin, 1976a). The availability of an antibody that recognizes an actin epitope in basal body-associated filaments will make possible developmental studies that can determine whether a causal relationship exists between actin filament formation and basal body migration during morphogenesis. A role for actin filaments in directing basal body migration during ciliogenesis has been proposed by other investigators (Lemullois *et al.*, 1987; Tamm and Tamm, 1988).

Actin Is Associated with *Tetrahymena* Mucocysts

In this study, I have demonstrated by immunogold labeling that an affinity-purified, anti-actin antibody localized to *Tetrahymena* mucocysts docked at the cell surface. Colloidal gold particles were located throughout the mucocyst matrix which suggested an extensive distribution of actin epitopes. Specifically, the antibody localized to filaments associated with mucocyst matrix material. Immunoblotting and quantitative analysis of gold

particle distribution were used to further demonstrate the specificity of the antibody for actin in the mucocyst. Based on these data, it is concluded that actin filaments enmesh mucocyst material.

Tetrahymena contains approximately 5,000 mucocysts (Wolfe, 1988). Therefore, actin is probably a more abundant protein in *Tetrahymena* than previously reported (Hirono *et al.*, 1989). Actin is highly susceptible to degradation which could account for the relatively low yields of the protein when whole cells are used for purification studies. If most of the actin in *Tetrahymena* is located in the cortex, isolated cortical fractions would be a better starting material for actin purification. Isolated cortical fractions would offer a further advantage of having a lower contaminating protease concentration than whole cell homogenates.

Effects of cytochalasin on mucocyst structure

Cytochalasin is known to disrupt actin filaments (Hartwig and Stossel 1979; Schliwa, 1982). However, I did not detect any apparent change in either mucocyst structure or the pattern of antibody labeling in cytochalasin D-treated cells. If the drug severed the filament network in docked mucocysts, the highly condensed mucocyst matrix, enclosed by the mucocyst membrane, would have probably remained intact, and the severed actin filaments would have remained accessible to the antibody.

Exocytosis of Tetrahymena mucocyst material

The ultrastructure of the *Tetrahymena* mucocyst and its secretory pathway have been extensively described (Satir *et al.*, 1973; Tokuyasu and Scherbaum, 1965). The schematic diagram in Fig. 26 depicts the exocytosis of *Tetrahymena* mucocyst material. Three distinct membranes can be identified

in the *Tetrahymena* cortex (Allen, 1967; Tokuyasu and Scherbaum, 1965). Two outer membranes are represented as closely spaced parallel lines. The outermost membrane of this pair is the plasma membrane. The third and innermost membrane directly covers the cytoplasm and contains the initial docking site for the mucocyst (Fig. 26a). Activation of a mucocyst leads to fusion of the mucocyst membrane with the plasma membrane, decondensation and expansion of the crystalline material, and the change from spindle-shaped to spherical with a substantial increase in membrane surface area (Fig. 26b). In the region of the fusion pore, the middle membrane fuses with the innermost membrane to form an alveolus (Fig. 26b). Mucocyst contents are discharged through the expanded exocytotic fusion pore (Fig. 26c). The fusion pore closes, and the empty mucocyst vacuole (discharged mucocyst) is left in the cytoplasm (Fig. 26d). Discharged contents are either dispersed (Fig. 26c) or lodged at the cell surface (Fig. 26d).

A possible role for an actomyosin system in exocytosis

The primary significance of these results is their relevance to a possible role for an actomyosin system in the discharge of secretory vesicle contents through the cell surface. Mucocyst discharge is both rapid and forceful. Tokuyasu and Scherbaum (1965) described the force that propels mucocyst contents through the exocytotic pore as "self-propelling". This self-propelling force could be generated by contractile events involving a cytoskeletal actomyosin system associated with the mucocyst matrix. Mucocyst discharge is preceded by expansion of mucocyst matrix material and the change from spindle-shaped to spherical with a substantial increase in membrane surface area. Expansion of the matrix material could include

expansion of the actin meshwork, possibly by unwinding of actin filament bundles which could create a new spatial arrangement of contractile units within the mucocyst matrix. The new spatial arrangement would increase the distance over which a contractile event could occur and therefore increase the amount of force generated. We can further speculate that the force generated by contraction of the actin meshwork in the mucocyst matrix could propel mucocyst material through the fusion pore with sufficient momentum to carry the bound actin with it. Complete dispersal of discharged mucocyst contents would probably require the simultaneous depolymerization or severing of the actin filaments in order to dissociate them from the mucocyst material.

Although there is no evidence for contraction involving mucocyst-associated actin filaments, there is evidence for discharge of mucocyst -associated actin filaments during the exocytosis of mucocyst material. Immunogold labeling clearly showed that dense filamentous material, heavily labeled with colloidal gold particles and presumed to be discharged mucocyst material, was lodged on the cell surface near an exocytotic site (Fig. 17b). Furthermore, both immunogold labeling and quantitative analysis of gold particle distribution showed that discharged mucocysts did not contain a significant number of actin epitopes (Fig. 17b, table 1). If the mucocyst actin meshwork had depolymerized to G-actin during exocytosis and remained in the discharged mucocyst, immunogold labeling would have detected it because the anti-actin antibody was capable of detecting both G and F-actin. Taken together, these observations support the conclusion that discharged mucocyst material contained actin filaments.

The existence of mucocyst-associated actin filaments raises the possibility that actomyosin systems play important roles in the exocytosis of

other secretory vesicles. For example, the mast cell secretory granule contains an actin filament network associated with the granule membrane (Nielsen, 1990). Although the function of this network is not known, it has been suggested that rearrangement of the network is probably required in order for exocytosis to occur. Future studies will undoubtedly refine our understanding of the role of actin in the exocytotic process and the relationship of mucocyst-associated actin to basal body-associated actin. Microinjection of antibodies is likely to be an important means of assessing the precise function of actin in exocytosis and basal body movement.

Actin Localizes to the Macronucleus

Stress conditions such as heat shock or DMSO treatment can induce the formation of intranuclear actin filament bundles in rat fibroblasts (Welch and Suhan, 1985) and in *Tetrahymena* (Hirono *et al.*, 1987). In *Tetrahymena*, the diameter of this actin filament aggregate is about 300 nm (Hirono *et al.*, 1987). The function of the stress-induced intranuclear actin filaments remains unclear. In the present study, labeling of macronuclear actin filaments under non-stress conditions strongly suggests that under conditions of stress, pre-existing nuclear actin--either as F-actin or G-actin--is recruited to form the filament bundles.

Other Cortical Contractile Systems in Ciliates

Several studies have described filamentous, contractile systems in the ciliate cortex. In *Paramecium*, the innermost region of the cytoskeleton contains an infraciliary lattice, a contractile network at the proximal ends of basal bodies (Garreau de Loubresse *et al.*, 1988, 1991). In *Isotricha*, the outer region of the cortex is separated from the endoplasm by a contractile

fibrillar network known as the ecto-endoplasmic boundary (Vigues *et al.*, 1984). Vorticellid ciliates contain a contractile organelle, the spasmoneme, which consists of calcium-binding polypeptides known as spasmins (Amos, 1975). The contractile systems in *Paramecium, Isotricha,* and vorticellids appear to be related by 20 kDa, acidic, calcium-binding proteins which have been suggested as modulators of contractility in each system (Garreau de Loubresse *et al.*, 1988, 1991; Vigues *et al.*, 1984; Amos, 1975). The 20 kDa proteins in ciliates are probably related to centrin/caltractin, a family of calcium-binding, algal proteins described by Salisbury *et al.*, (1989) and by Huang *et al.*, (1988). The present study strenghtens the proposition of contractile systems in ciliates by providing ultrastructural evidence for the localization of actin in basal body-cage complexes and in the mucocyst. The precise relationship between the putative contractile system associated with *Tetrahymena* basal bodies and mucocysts and the contractile systems in *Paramecium* and other ciliates must await further characterization of the ciliate cortex.

Figure 1. Diagrammatic representation of the cortical morphology of *Tetrahymena* as revealed by silver nitrate preparations. The meridional lines represent the somatic rows of cilia. The oral apparatus consists of three membranelles (M_1, M_2, M_3) and an undulating membrane (UM). The oral primordium for the posterior division product appears in the area designated as PS (primordium site).

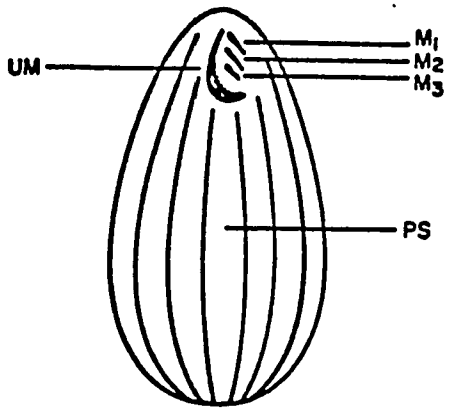
UM
M1
M2
M3
PS

Figure 2. A diagram, based on electron micrographs of whole mount and thin section preparations, showing the relationship between oral apparatus basal bodies (represented as open circles) and the various fiber groups (represented) as solid lines). Each membranelle (M1) consists of three rows of hexagonally arranged, ciliated basal bodies. The undulating membrane (UM) consists of two rows of basal bodies of which only one row is ciliated. *Membranellar connectives* (MC) interconnect the three membranelles. The anterior end of each membranelle is connected to the undulating membrane by *cross connectives* (PC). The oral ribs (OR) originate at the undulating membrane and join with fibers from the third membranelle to form the deep fiber (DF).

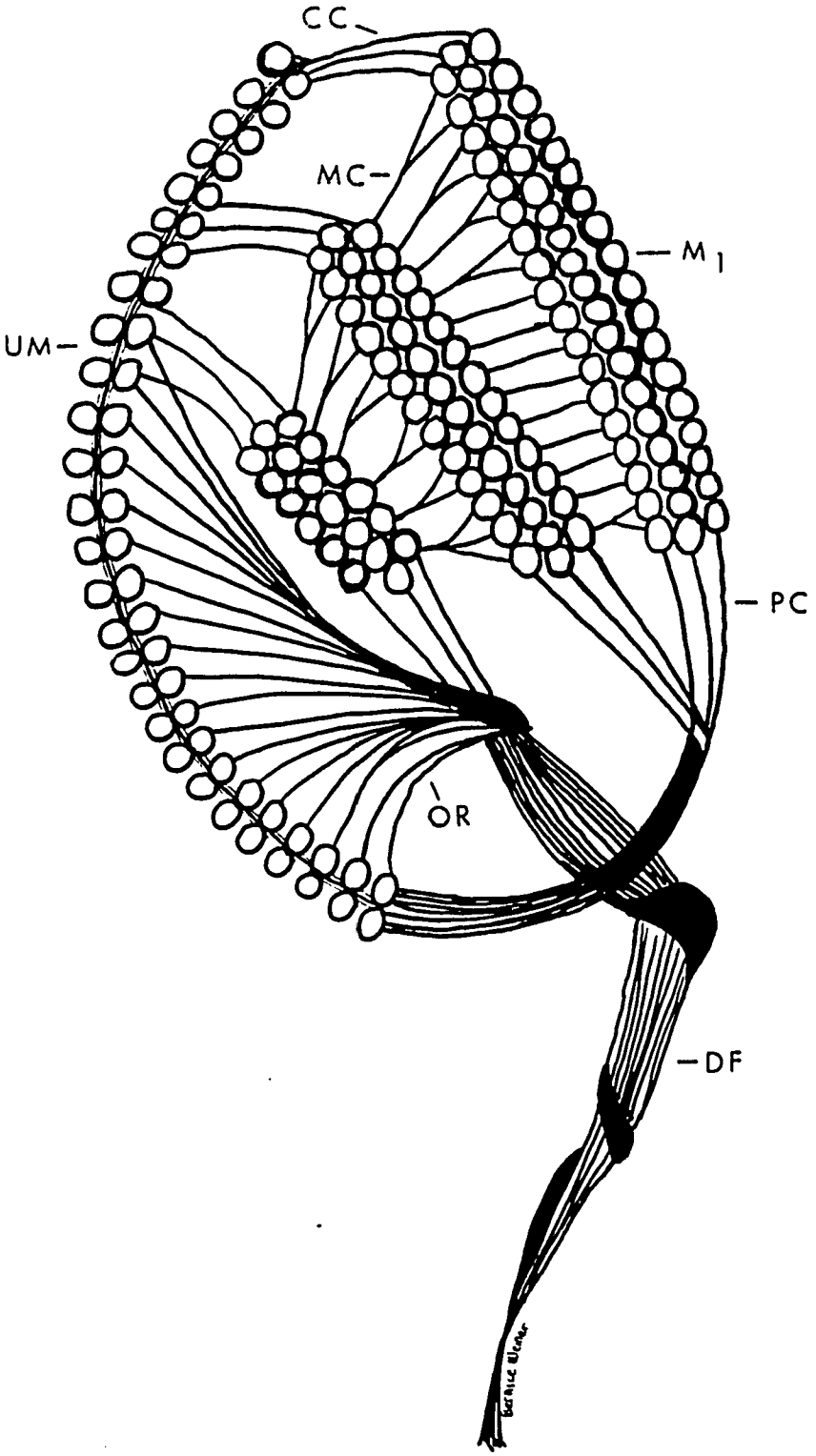
CC
MC
M1
UM
PC
OR
DF

Figure 3. All lanes are from the same gel. Lane a: Coomassie Blue-stained gel containing molecular mass standards. Lane b: Coomassie Blue-stained gel containing 75 μg total oral apparatus protein (T, tubulins; A, actin). Lane c: Immunoblot containing 300 μg total oral apparatus protein stained with a 1:100 dilution of anti-oral apparatus antiserum. The arrowhead denotes actin. Lane d: Immunoblot containing 300 μg total oral apparatus protein stained with a 1:50 dilution of preimmune serum.

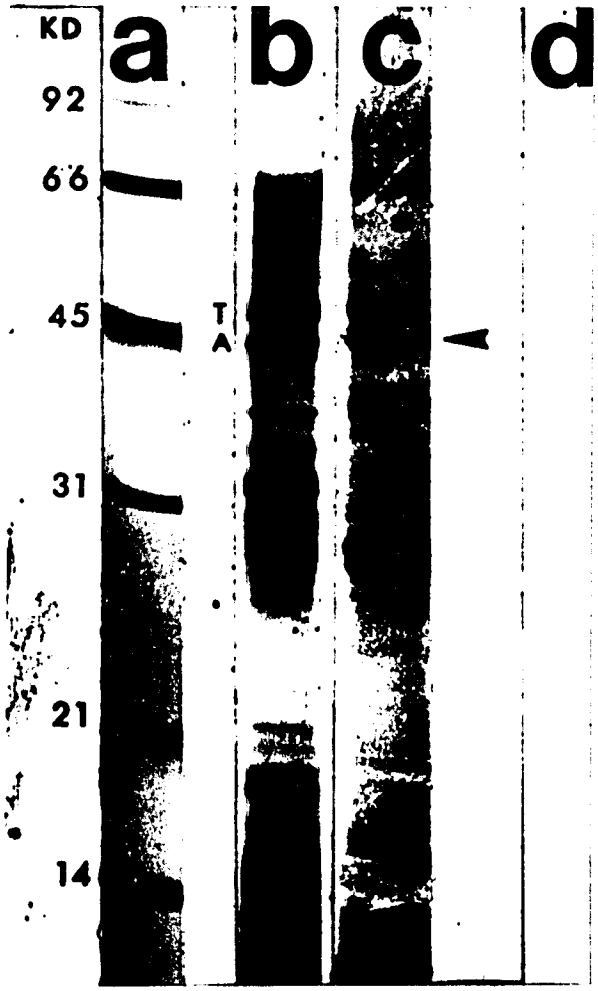
KD
a
b
c
d
92
66
45
31
21
14
T
A

Figure 4. All lanes are from the same gel. Lane a: Coomassie Blue-stained gel containing molecular mass standards. Lane b: Coomassie Blue-stained gel containing 5 μg chicken muscle actin. Lane c: Immunoblot containing 20 μg chicken muscle actin stained with a 1:100 dilution of anti-oral apparatus antiserum. Lane d: Immunoblot containing 20 μg chicken muscle actin stained with a 1:10 dilution of affinity-purified anti-*Tetrahymena* actin antibody.

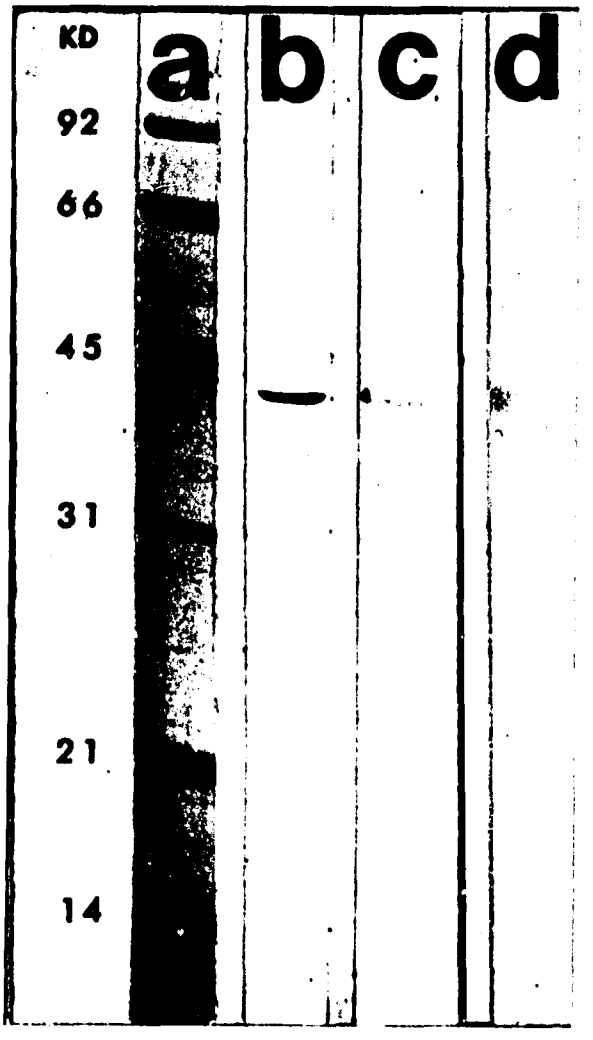
KD
a
b
c
d
92
66
45
31
21
14

Figure 5. Lane A: Coomassie Blue-stained gel containing molecular mass standards. Lane B: Coomassie Blue-stained gel containing chicken muscle myosin light chain polypeptides. Lane C: immunoblot containing chicken muscle myosin light chain polypeptides probed with anti-*Tetrahymena* oral apparatus antiserum. The antibody cross-reacts with the 25 kDa and 18 kDa muscle myosin light chain proteins.

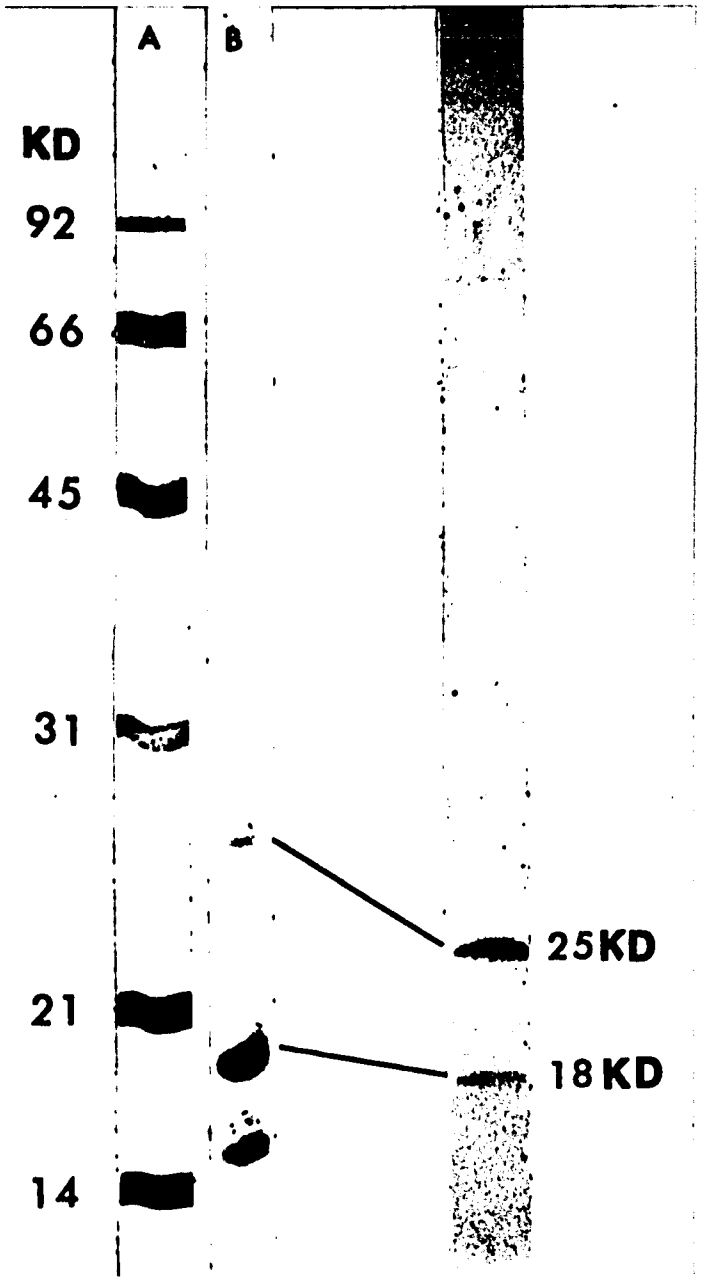
A
B
KD
92
66
45
31
21
14
25KD
18KD

Figure 6. All lanes are from the same gel. Lane a: Coomassie Blue-stained gel containing molecular mass standards. Lane b: Coomassie Blue-stained gel containing 75 μg total oral apparatus protein. Lane c: Immunoblot containing 300 μg total oral apparatus protein stained with a 1:10 dilution of affinity-purified anti-*Tetrahymena* actin antibody. Lane d: Immunoblot containing 300 μg total oral apparatus protein stained with a 1:10 dilution of affinity-purified anti-chicken muscle actin antibody. Lane e: Immunoblot containing 300 μg total oral apparatus protein stained with a 1:10 dilution of actin-adsorbed anti-*Tetrahymena* actin antibody.

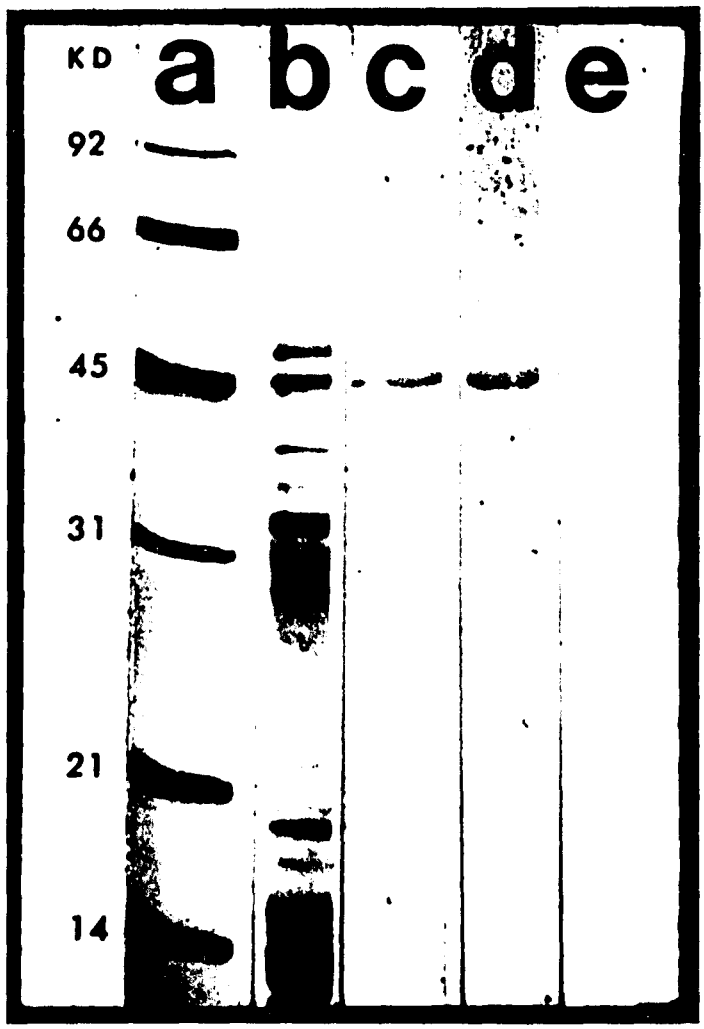
KD
a
b
c
d
e
92
66
45
31
21
14

Figure 7. All lanes are from the same gel. Lane A: Coomassie Blue-stained gel containing molecular mass standards. Lane B: Coomassie Blue-stained gel containing total oral apparatus proteins. Lane C: Immunoblot containing total oral apparatus proteins stained with affinity-purified anti-*Tetrahymena* myosin light chain-like antibody. The antibody cross-reacts with an 18 kDa oral apparatus protein.

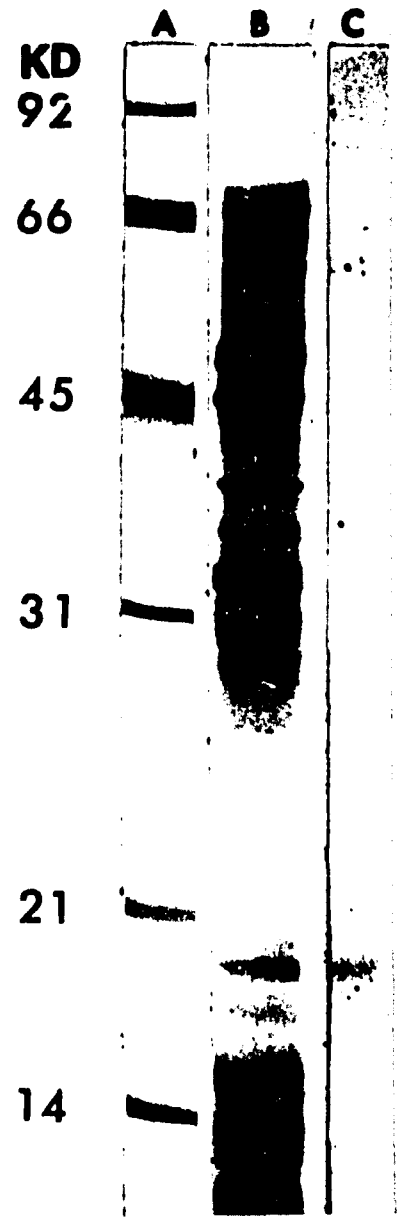
A
B
C
KD
92
66
45
31
21
14

Figure 8. a: Indirect immunofluorescence staining of *Tetrahymena* with a 1:20 dilution of affinity-purified anti-*Tetrahymena* actin antibody. The antibody localized to somatic basal bodies which are the bright longitudinal rows on the cell surface, and to the oral apparatus, which is a bright curved band at the anterior end of each cell. b: Preimmune serum control was photographed at the same exposure as (a). Bar= 5 μm

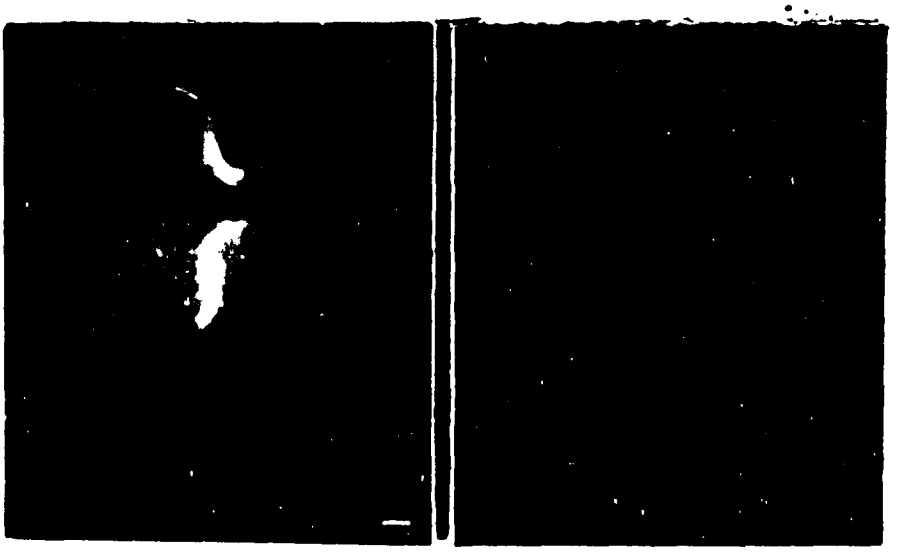

a b

Figure 9. In situ localization of affinity-purified anti *Tetrahymena* actin antibody. The secondary antibody was linked to 15 nm colloidal gold particles. Somatic basal bodies are arranged in longitudinal rows in which a basal body alternates with a mucocyst. In this section, two basal bodies and two empty mucocyst sites are visible. One of the basal bodies is not completely in the plane of section. Colloidal gold particles decorate the basal body wall, basal plate region, and filaments (arrow) at the proximal end of the basal body. In addition, colloidal gold decorates filaments in the cytoplasm. Note the line of gold particles in each mucocyst docking area. Bar= 0.2 μm

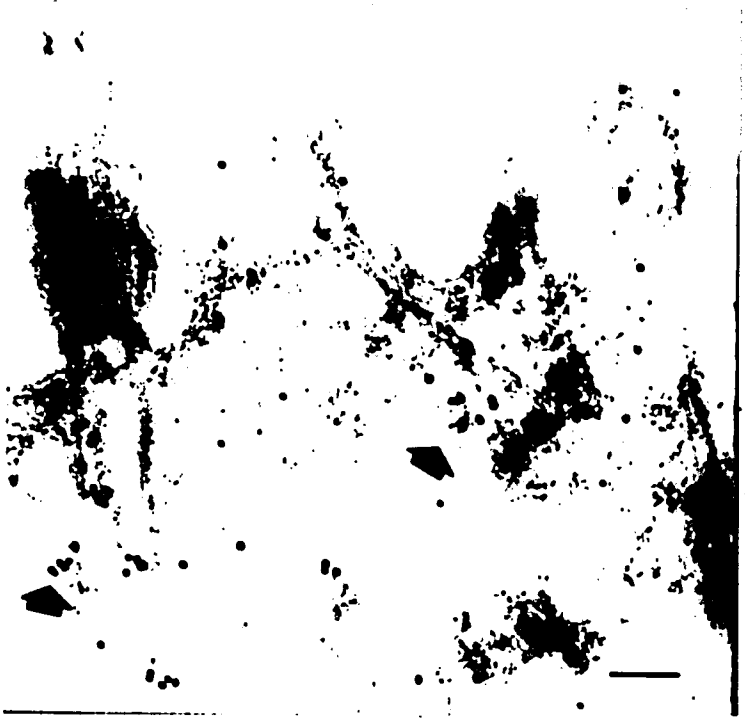

Figure 10. A detailed view of the basal body cage-complex. (BP) Basal Plate. The basal plate consists of interwoven fibers at the end of the basal body cylinder closer to the cell surface. The basal plate marks the transition from basal body to cilium, and it forms the top of the basal body cage. (CW) Cage Wall. The cage wall around oral basal bodies consists of a filamentous partition connected to the basal body wall by a network of thin filaments. (BBW) Basal Body Wall. The basal body walls consist of the microtubule boundaries of the entire cylinder except the basal plate. (PF) Proximal Filaments. Proximal filaments at the end of the basal body cylinder farther from the cell surface form the base of the basal body cage. Bar= 0.1 μm

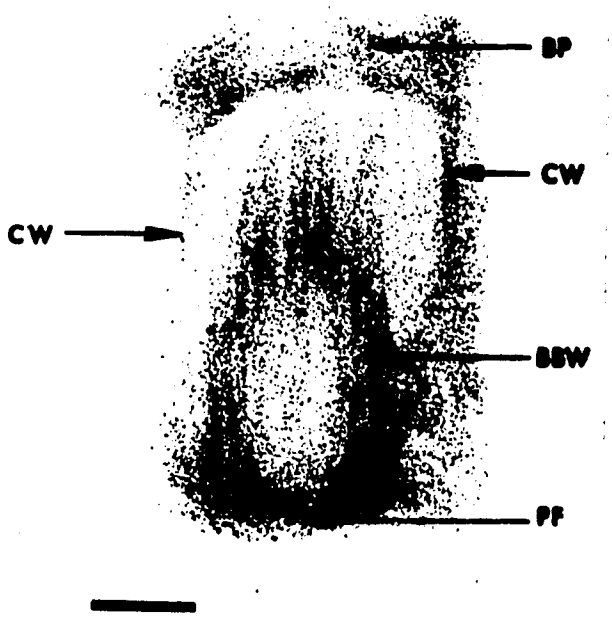
BP
CW
CW
BBW
PF

Figure 11a. A longitudinal section through basal bodies in an isolated oral apparatus. Although each basal body is enclosed by a filamentous cage, the walls (arrowheads) of a single cage are in the plane of section in this figure. The microtubules (curved arrow) at the base of the cage interconnect rows of basal bodies within the oral apparatus. Bar= 0.4 μm

Figure 11b. This micrograph shows the close association between basal body microtubules and filaments in the oral apparatus. The plane of section is through the region where basal body microtubules (arrows) are connected to cage walls (arrowheads) by a network of thin filaments, some of which are 5-6 nm in diameter. Numerous filaments at the distal region appear to be continous with the walls of the basal body cages. The dense network of fibers at the proximal region form the base of the cage from which emanate accessory microtubules. Bar= 0.4 μm

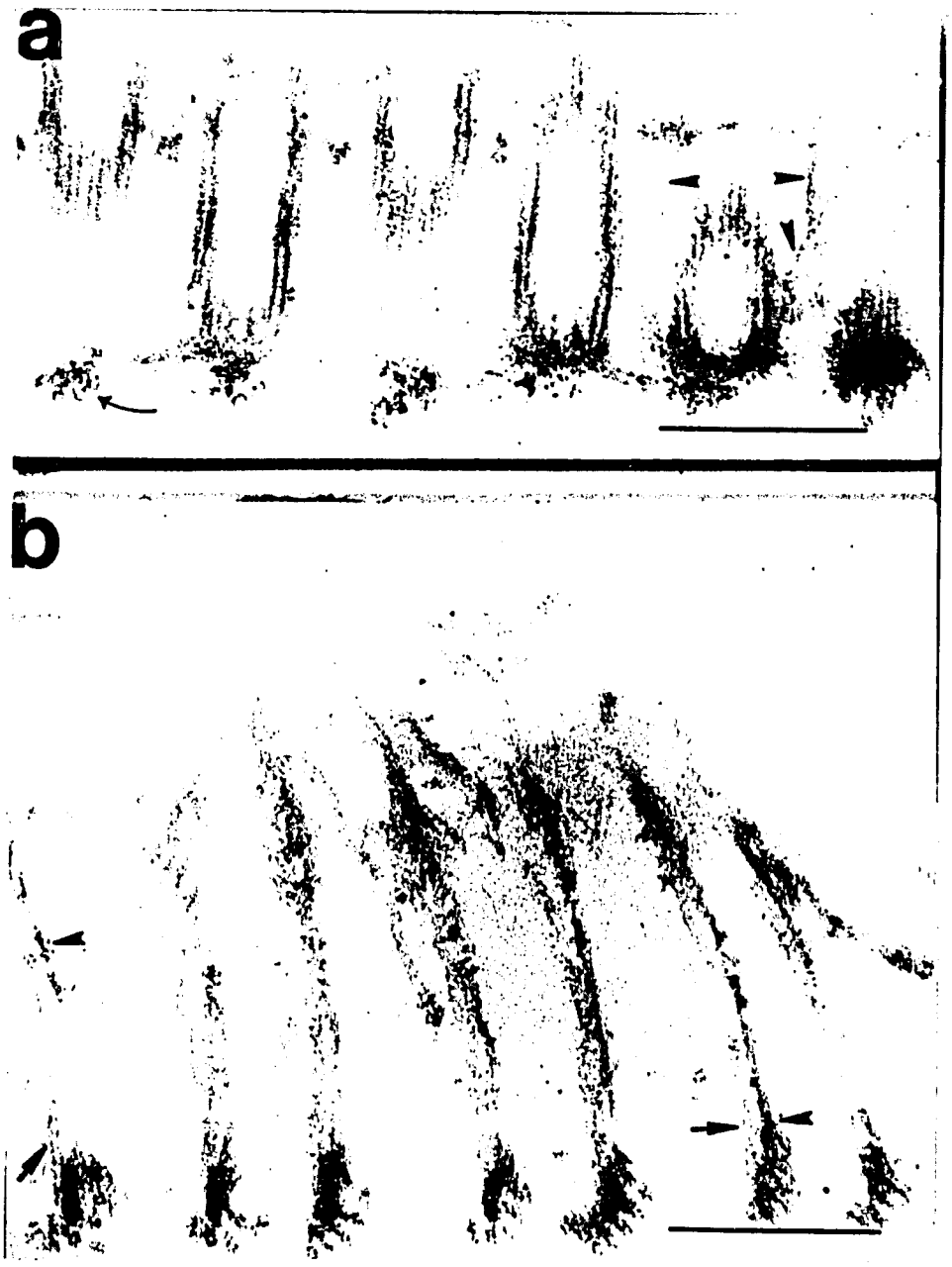
a
b

Figure 12. A transverse section through basal bodies in an isolated oral apparatus labeled with affinity-purified anti-*Tetrahymena* actin antibody followed by IgG secondary antibody linked to 15 nm colloidal gold particles. There is very low background staining. Colloidal gold particles are closely associated with basal body microtubules. Bar= 0.4 μm

Figure 13. A detailed view of basal bodies and cage walls in an isolated oral apparatus stained with affinity-purified anti-*Tetrahymena* actin antibody followed by secondary antibody linked to 15 nm colloidal gold particles. a: Colloidal gold particles decorate the entire length of the basal body wall from the basal plate to the proximal-end filaments. b: Although basal bodies are not in the plane of section, cage walls are visible and labeled with colloidal gold. Bar= 0.4 μm

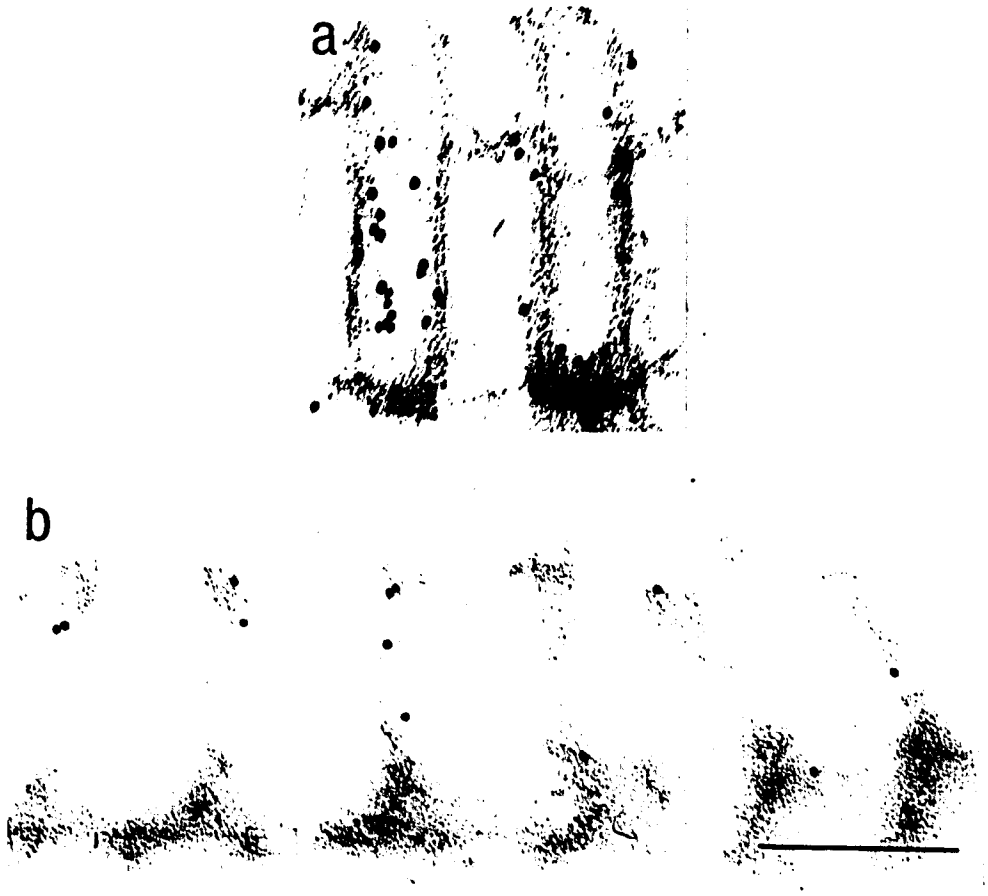
a
b

Figure 14. A transverse section through basal bodies in an isolated oral apparatus labeled with affinity-purified, anti-*Tetrahymena* actin antibody followed by secondary antibody linked to 15 nm colloidal gold particles. Colloidal gold particles are closely associated with regions of the basal body wall where filaments project (arrows). These filaments connect the basal body wall with the cage wall (arrowhead). The rosettes around basal bodies are formed from interwoven filaments of the basal plate which forms the top of the cage. The right margin of the micrograph shows labeling of basal plate filaments. The long filament bundles that connect one row of basal bodies with another row are also immunoreactive with the antibody. Bar= 0.4 μm

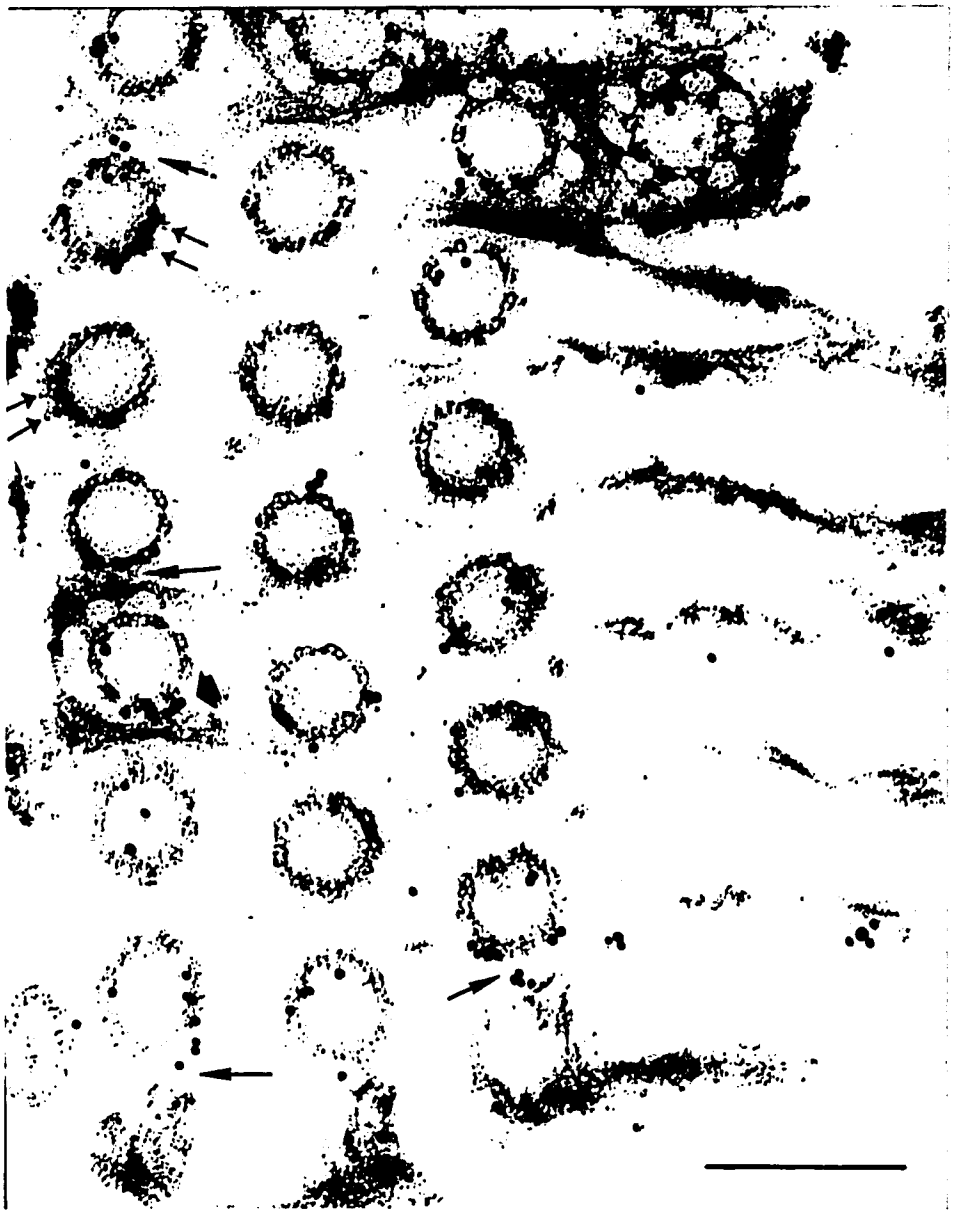

Figure 15. A transverse section through basal bodies in an isolated oral apparatus. The primary antibody was affinity-purified, actin-adsorbed, anti-*Tetrahymena* actin antibody. The secondary antibody was anti IgG linked to 15 nm colloidal gold particles. Only a few random gold particles are seen in this micrograph. Bar= 0.4 μm

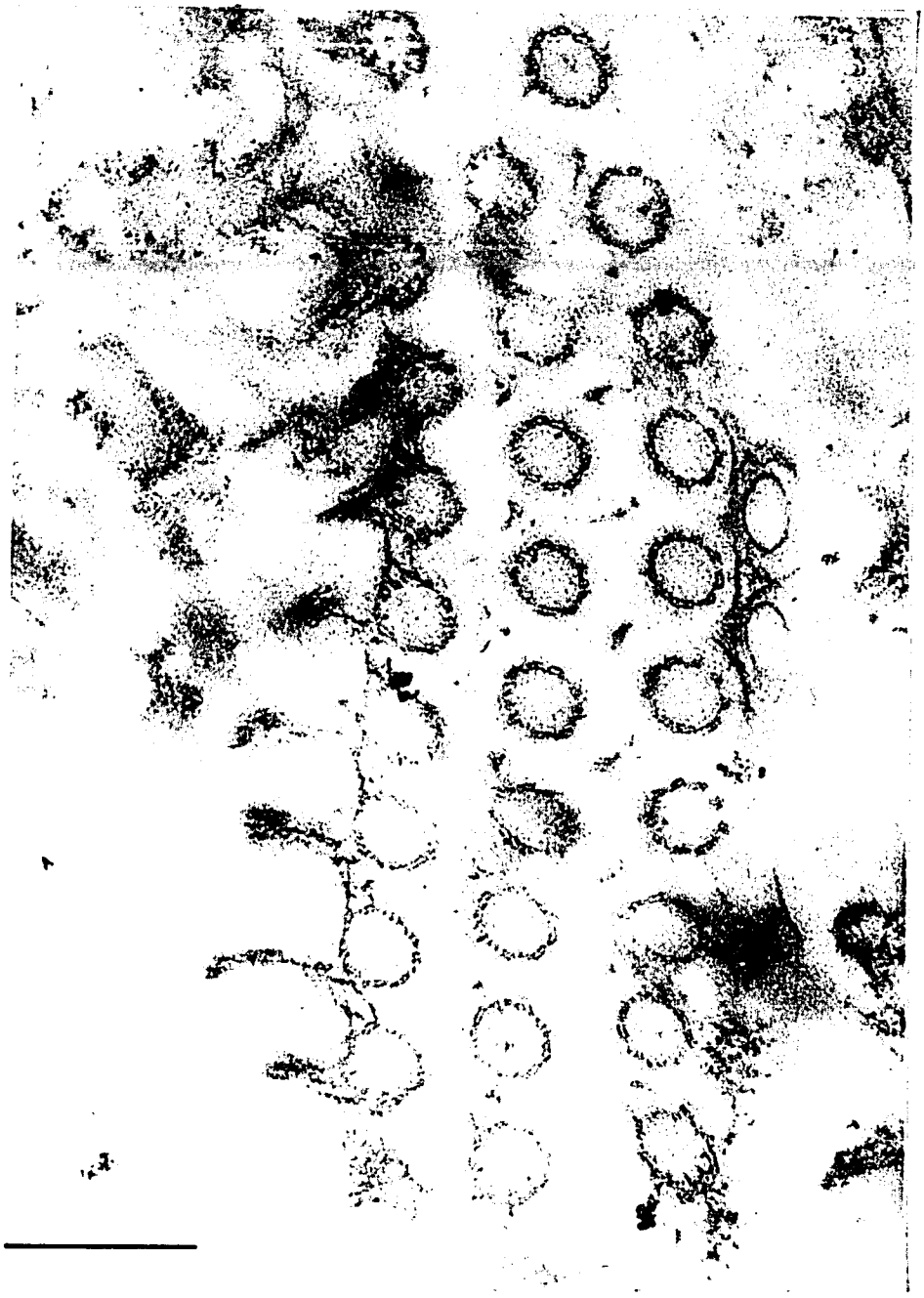

Figure 16. Immunogold localization of actin to mucocysts *in situ*. This section was labeled with affinity-purified, anti-*Tetrahymena* actin antibody followed by secondary antibody linked to 15 nm colloidal gold particles. Mucocysts (arrowheads) are docked at the cell surface, and are heavily labeled with colloidal gold particles. The mitochondrion (Mi) shows only background labeling. Bar= 0.14 μm

Figure 17. Immunogold localization of actin to mucocysts *in situ*. Sections were labeled with affinity-purified, anti-actin antibody followed by secondary antibody linked to 15 nm colloidal gold particles. a: Colloidal gold particles decorate a mucocyst docked at the cell surface. Note the filaments and the line of gold particles at the periphery of the mucocyst material (arrowhead). Bar= 0.13 μm b: Discharged mucocyst contents, heavily labeled with colloidal gold particles, are lodged at the outer cell surface above the exocytotic fusion pore site. The mucocyst material contains filaments decorated with colloidal gold particles (arrowhead). There is virtually no colloidal gold labeling in the discharged mucocyst (dm). Bar= 0.22 μm

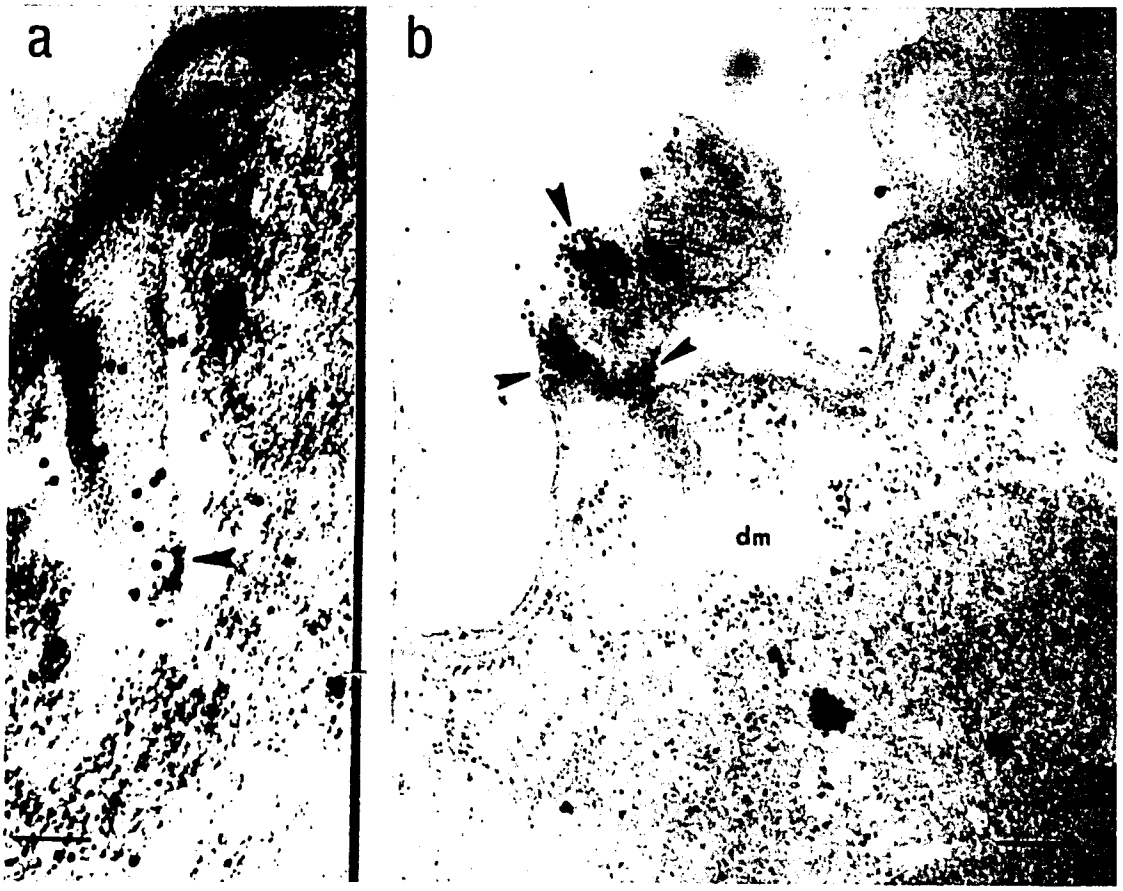
a
b
dm

Figure 18. Control experiment for *in situ* localization of actin to mucocysts. This section was labeled with preimmune serum followed by secondary antibody linked to 15 nm colloidal gold particles. There are only a few random gold particles. Bar= 0.2 μm

Figure 19. This section through a *Tetrahymena* cell shows the general organization of the macronucleus (MN) and its spatial relationship to the oral apparatus (OA). Bar= 0.2 μm

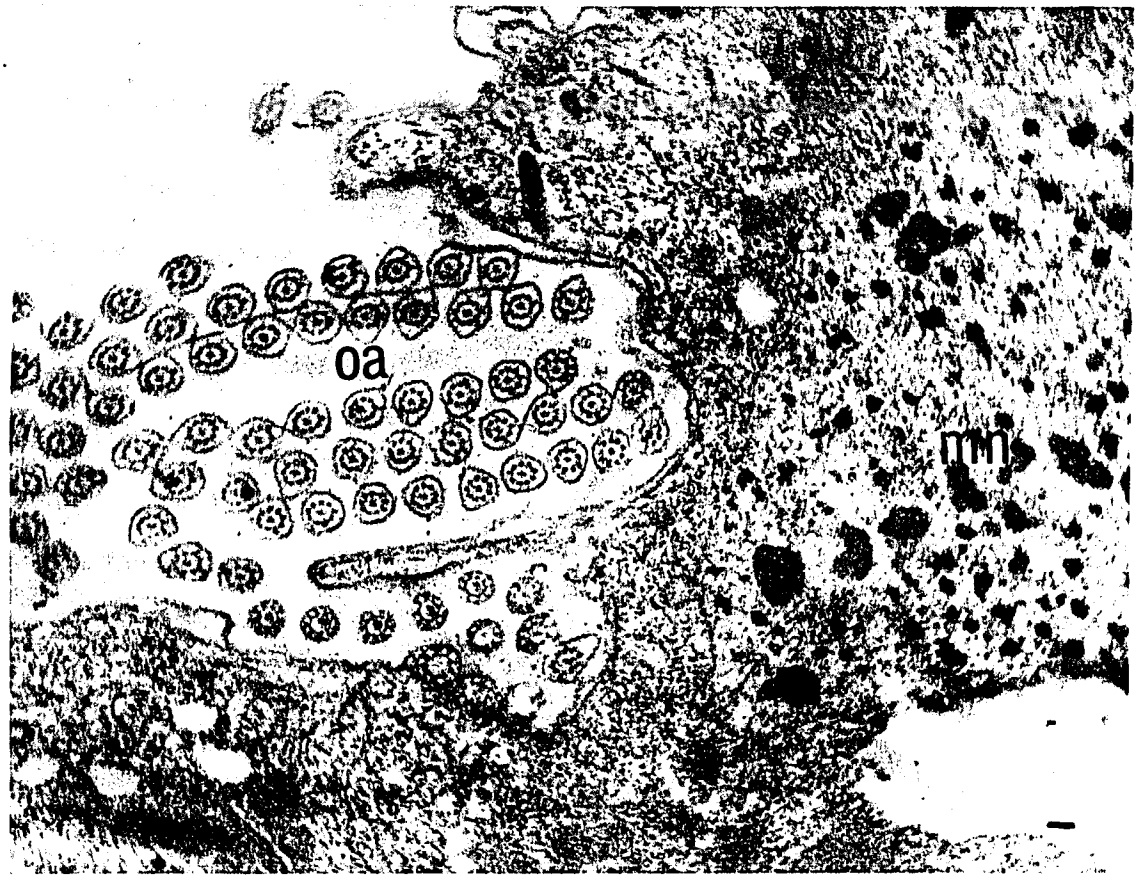
oa
mi

Figure 20. A cross-section through a portion of the macronucleus. This section was labeled with anti-*Tetrahymena* actin followed by 15 nm colloidal gold linked anti-IgG secondary antibody. The antibody labeled filaments (arrows) located between the dense chromatin bodies (arrowheads).

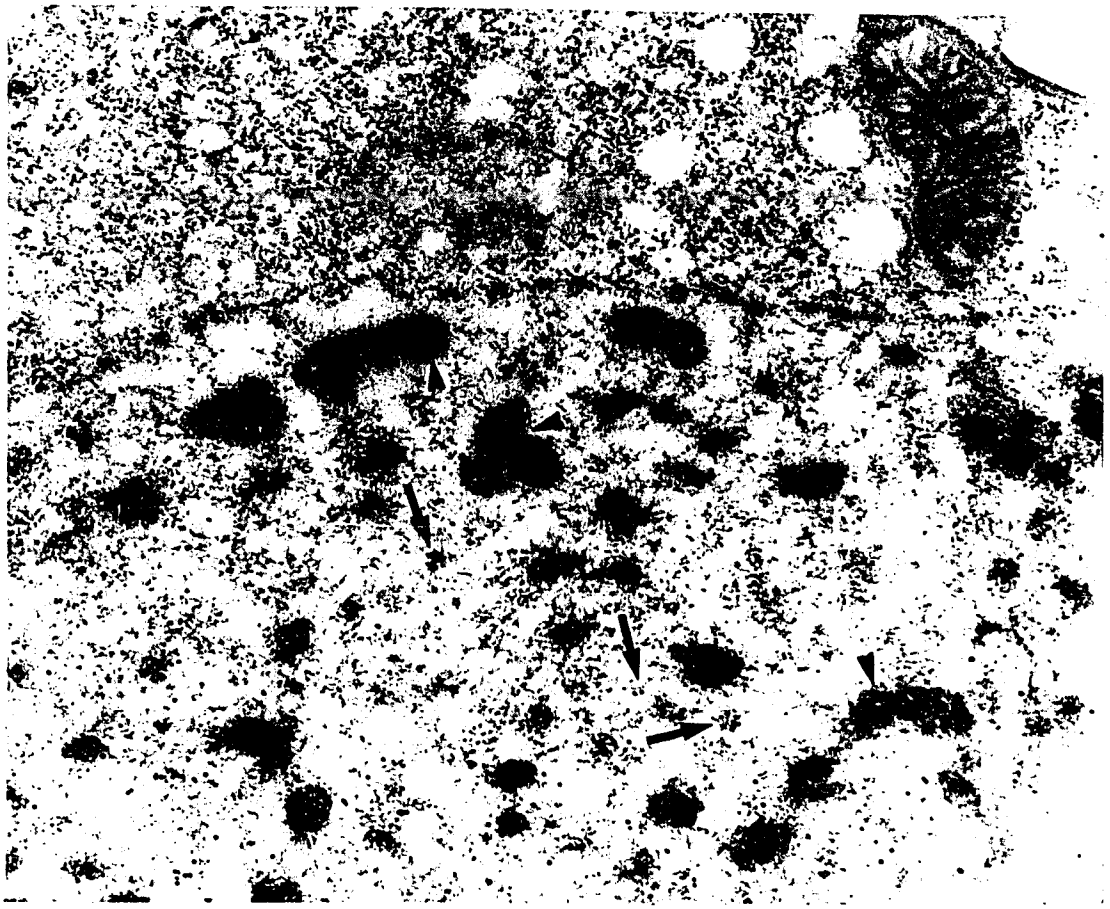

Figure 21. A longitudinal section through basal bodies in an isolated oral apparatus. This section was labeled with affinity-purified, anti-*Tetrahymena* 18 kDa antibody followed by secondary antibody linked to 15 nm colloidal gold. Colloidal gold particles are closely associated with basal body microtubules (arrows), proximal filaments (arrowhead), and distal filaments (open arrow). Bar= 0.2 μm

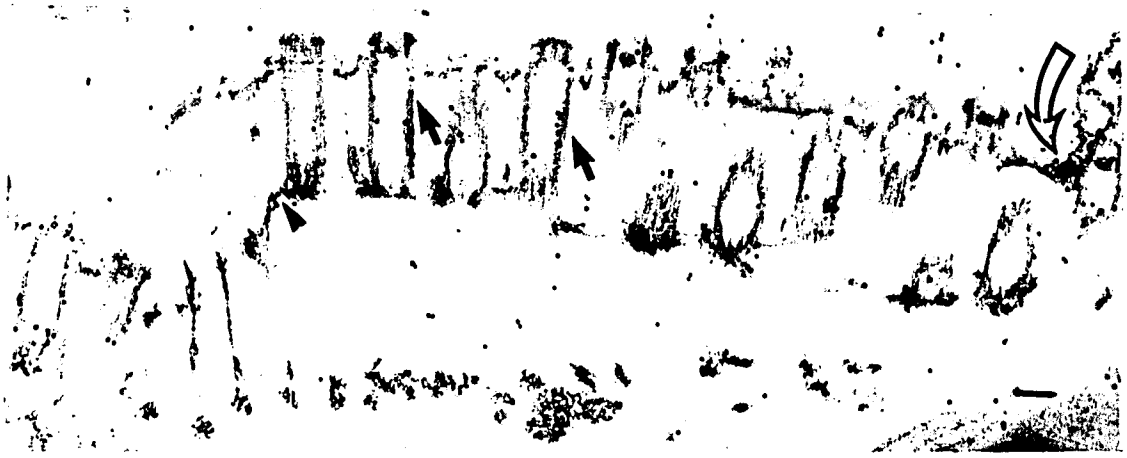

Figure 22. A longitudinal section through basal bodies in an isolated oral apparatus. This section was labeled first with affinity-purified, anti-*Tetrahymena* actin antibody followed by 15 nm colloidal gold anti-IgG, and then with affinity-purified anti-18 kDa antibody followed by 5 nm colloidal gold anti-IgG. This micrograph shows that the anti-actin (15 nm particles, arrow) and the anti-18 kDa antibody (5 nm particles, arrowhead) colocalize to filaments closely associated with basal body microtubules. Bar= 0.4 μm

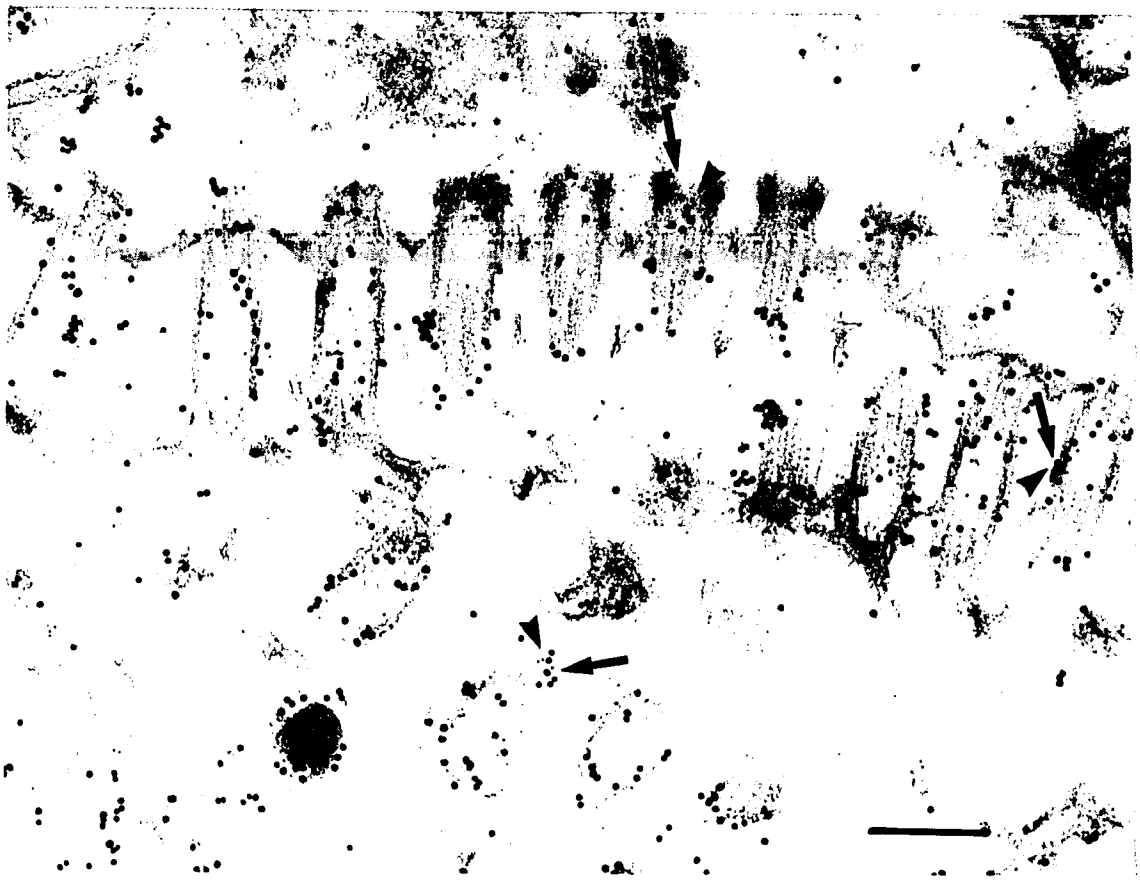

Figure 23. A cross-section through basal bodies in an isolated oral apparatus. This section was labeled first with affinity-purified, anti-*Tetrahymena* actin followed by 15 nm colloidal gold anti-IgG, and then with affinity-purified, anti-18 kDa antibody followed by 5 nm colloidal gold anti-IgG. This micrograph shows that the anti-actin (15 nm particles, arrow) and the anti-18 kDa antibodies (5 nm particles, arrowhead) colocalize to regions of the basal body where filaments project. Bar= 0.2 μm

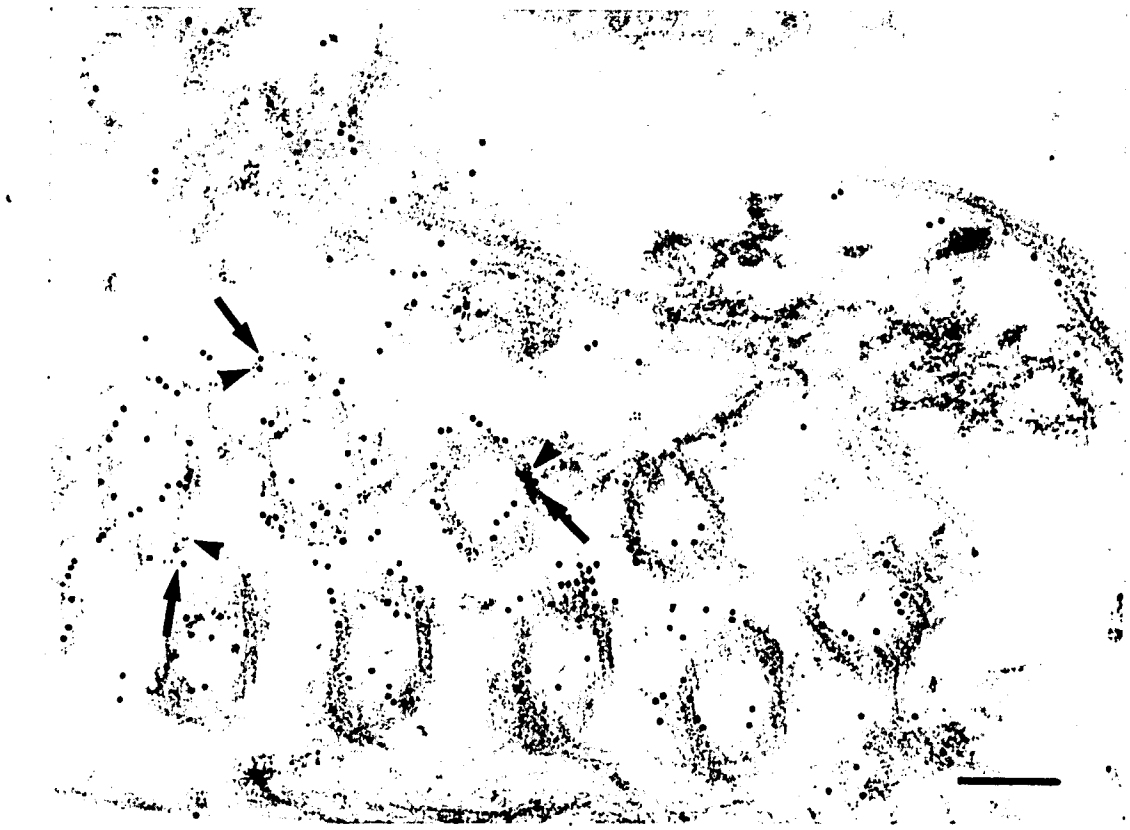

Figure 24. Control for double labeling experiment. A longitudinal section through a row of basal bodies in an isolated oral apparatus. This section was incubated with anti 18 kDa followed by secondary antibody linked to 15 nm colloidal gold particles. This section was subsequently incubated with unlabeled anti-IgG followed by IgG linked to 5 nm colloidal gold particles. Only a few random 5 nm gold particles can be seen in this micrograph. The virtual absence of 5 nm particles in this micrograph demonstrates the absence of a significant number of unreactive sites after incubation in anti-18 kDa antibody. Bar= 0.2 μm

Figure 25. Control for double labeling. A longitudinal section through a row of basal bodies in an isolated oral apparatus incubated with anti 18 kDa followed by secondary antibody linked to 15 nm colloidal gold particles. This section was subsequently incubated with unlabeled anti-IgG followed by IgG linked to 5nm colloidal gold particles. Only a few random 5 nm gold particles can be seen in this micrograph. The virtual absence of 5 nm particles in this micrograph demonstrates the absence of a significant number of unreactive sites remaining after incubation in anti-18 kDa antibody. Bar= 0.4 μm

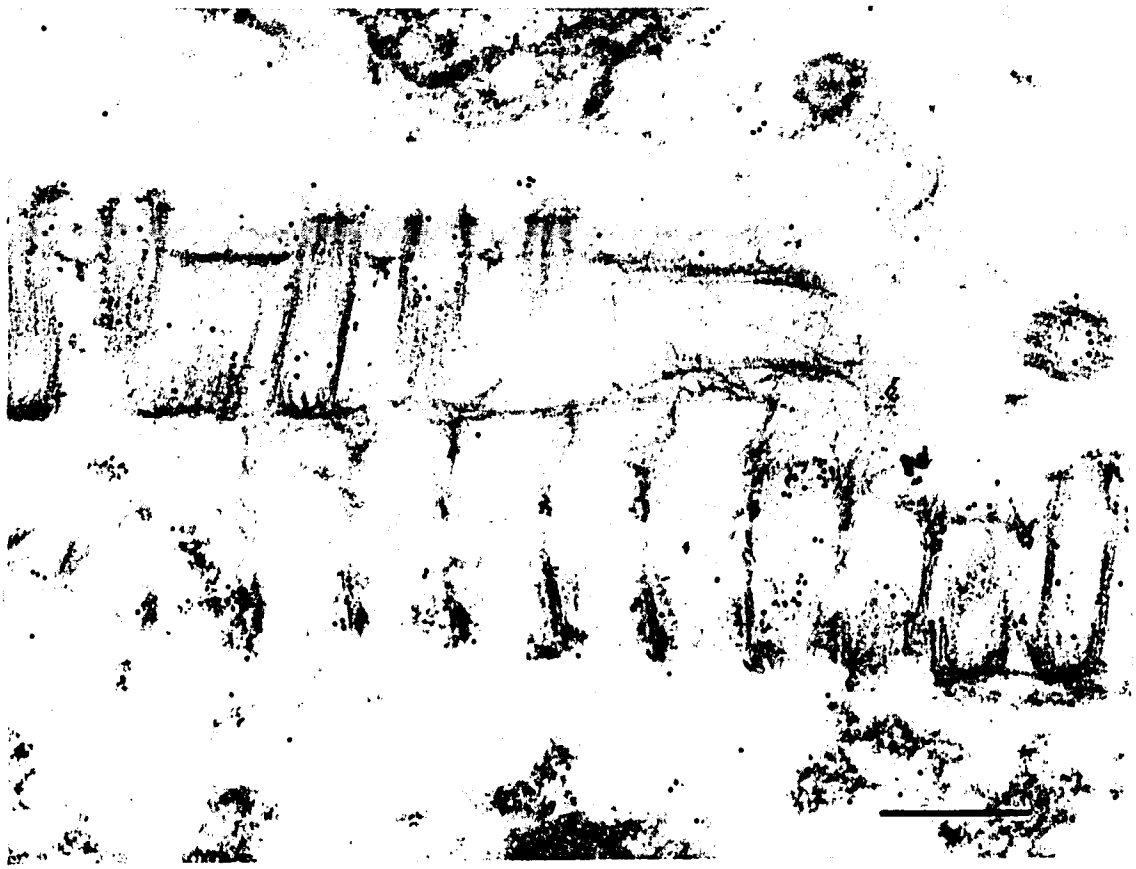

Figure 26. Diagrammatic representation of exocytosis of mucocyst material. a: There are three cortical membranes in *Tetrahymena*. The outer and inner pellicular membranes are represented by the two closely spaced horizontal lines. The third membrane, the cytoplasmic membrane, contains the initial docking site for the mucocyst. b: The mucocyst membrane has fused with the outer pellicular membrane, forming a fusion pore which leads into the interior of the expanded, spherical mucocyst. In the region of the fusion pore, the inner pellicular membrane fuses with the cytoplasmic membrane. The membrane surface area of the expanded mucocyst is considerably greater than the membrane surface area of the spindle-shaped mucocyst. The expanded mucocyst material is depicted as being fully enmeshed by actin filaments. c: The force generated by the contraction of actin filaments is proposed to force mucocyst material and the bound actin filaments through the fusion pore. d: Some of the discharged mucocyst material, still enmeshed by actin filaments, can remain lodged on the outer cell surface even after closure of the fusion pore. The discharged mucucyst remains in the cytoplasm.

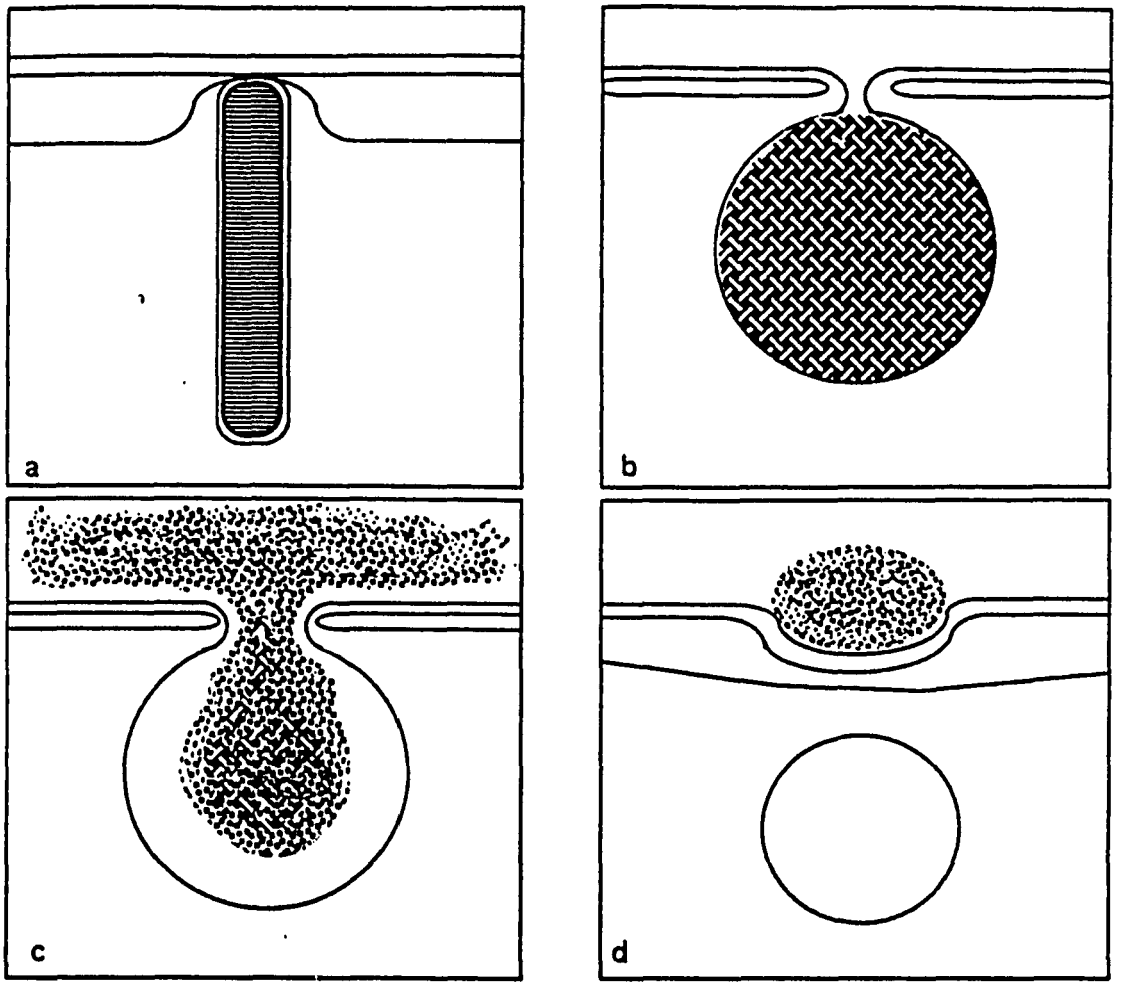
a
b
c
d

Table 1. Localization of Anti-Actin Antibodies in *Tetrahymena*

Region	Total Particles	Relative Density
Basal-Body Cage Complex	904	0.421 ± 0.05
Docked Mucocyst	648	0.303 ± 0.05
Discharged Mucocyst	27	0.012 ± 0.02
Cytoplasmic Filaments	296	0.128 ± 0.03
Macronucleus	199	0.094 ± 0.03
Plasma Membrane	78	0.031 ± 0.02
Mitochondrion	22	0.01 ± 0.02

Data analysis was achieved by placing a transparent sheet containing a point lattice directly over random electron micrographs. Lattice points coincident with colloidal gold particles over basal body-cage complexes, docked mucocysts, discharged mucocysts, cytoplasmic filaments, macronuclei, plasma membranes, and mitochondria were separately compiled. Relative colloidal gold particle densities over each region were computed as described by Weibel *et al.* (1966).

Table 2. Distribution of 15 nm and 5 nm Colloidal Gold Particles in a Double Label Control Experiment

15 nm particles per μm^2 basal body area	5 nm particles per μm^2 basal body area
138	4

Table 3. AMINO ACID COMPOSITION OF MYOSIN LIGHT CHAINS

Amino Acid	A1 (25 kDa)*	DTNB (18 kDa)*	(17/18 kDa)**
Acidic			
Asp	20.9	23.7	13.9
Glu	27.6	22.0	22.8
Basic			
Arg	4.1	5.9	8.4
Lys	18.8	16.0	10.2
	22.9	**21.9**	**18.6**
Hydrophilic			
Gly	11.9	12.6	5.7
Ser	5.5	5.9	6.7
Thr	7.9	8.9	6.1
	13.4	**14.8**	**12.8**
Hydrophilic (aliphatic)			
Val	9.8	8.8	7.9
Leu	13.4	9.6	12.2
Ile	9.2	10.1	8.5
Ala	23.2	13.1	7.5
Hydrophobic (aromatic)			
Phe	9.9	11.8	5.9
Tyr	1.0	2.0	6.2
	10.9	**13.8**	**12.1**
His	2.0	1.1	2.0
Pro	12.6	7.2	4.2
Total # Residues	184	166	128
Mol. Wt.	20,000	18,500	17,223

* Chicken muscle myosin light chains (Weeds and Lowey, J. Mol. Biol. 61:701)

** Putative *Tetrahymena* myosin light chain

SIGNIFICANCE

The results reported in this work are significant for the following reasons:

(1) They provide the first definitive ultrastructural evidence for actin in *Tetrahymena*. Specifically, actin was shown to be a component of basal body-associated filaments (cage-complex), mucocyst material, cytoplasmic filaments, and intranuclear filament bundles.

(2) They provide the first evidence for a myosin light chain-like polypeptide in *Tetrahymena*. This polypeptide was shown by immunoblotting and amino acid composition analysis to be similar to chicken muscle myosin 25 kDa and 18 kDa light chains.

(3) They provide evidence for myosin Mg^{2+}-ATPase activity within isolated oral apparatuses. The ATPase activity is consistent with a dynamic, functional actomyosin-based contractile system within this organelle complex.

Together, these experiments provide evidence for an actomyosin system associated with *Tetrahymena* basal bodies. This putative actomyosin system could induce changes in basal body orientation and, in doing so, influence oral apparatus morphogenesis. Moreover, changes in basal body orientation could alter the direction and/or magnitude of ciliary wave motion.

REFERENCES

Adams, R. J., Pollard, T. D. (1989). Binding of myosin I to membrane lipids. *Nature (Lond.).* **340**, 565-568.

Alberts, B., Bray, D., Lewis, J., Raff, M., Roberts, K., Watson, J. D. (1989a). The Cytoskeleton. In *Molecular Biology of the Cell.* (Garland Press) pp. 613-680.

Alberts, B., Bray, D., Lewis, J., Raff, M., Roberts, K., Watson, J. D. (1989b). Differentiated Cells and the Maintenance of Tissues. In *Molecular Biology of the Cell.* (Garland Press) pp. 951-1000.

Allen, R. D. (1967). Fine structure, reconstitution, and possible functions of components of the ciliate cortex of *Tetrahymena pyriformis. J. Protozool.* **14**, 553-565.

Amos, W. B., Routledge, L. M., Yew, F. (1975). Calcium-binding proteins in a vorticellid contractile organelle. *J. Cell Sci.* **19**, 203-213.

Arikawa, K., Williams, D. S. (1991). Alpha-actinin and actin in the outer retina: a double immunoelectron microscopic study. *Cell Mot. Cyto.* **18**, 15-25.

Baines, J. A., Korn, E. D. (1990). Localization of myosin IC and myosin II in *Acanthamoeba* castellanii by indirect immunofluorescence and immunogold electron microscopy. *J. Cell Biol.* **111**, 1895-1904.

Baines, I. C., Brzeska, H., Korn, E. D. (1992). Differential localization of *Acanthamoeba* myosin I isoforms. *J. Cell Biol.* **119**, 1193-1203.

Barden, J. A., Cooke, R., Wright, P. E., Dos Remedios, C. C. (1980). Proton nuclear magnetic resonance and electron paramagnetic resonance studies on skeletal muscle actin indicate that the metal and nucleotide binding sites are separate. *Biochemistry* **19**, 5912-5916.

Blackburn, E. H., Karrer, K. (1986). Genomic reorganization in ciliated protozoans. *Ann. Rev. Genet.* **20**, 501-521.

Bray, D. (1992a). Actin Filaments: Structure and Assembly. In *Cell Movements.* (Garland Publishing) pp. 75-92.

Bray, D. (1992b). Surface Contractions and Myosin. In *Cell Movements.* (Garland Publishing) pp. 107-122.

Bretscher, A. (1982). Characterization and ultrastructural role of the major components of the intestinal microvillus cytoskeleton. In *Cold Spring Harbor Symp. Quant. Biol.* **46**, 871-879.

Bretscher, A., Weber, K. (1978). Localization of actin and microfilament-associated proteins in the microvilli and terminal web of the intestinal brush border by immunofluorescence microscopy. *J. Cell Biol.* **79**, 839-845.

Brzeska, H., Lynch, T. J., Martin, B., Corigliano-Murphy, A., Korn, E. D. (1990a). Substrate specificity of *Acanthamoeba* myosin I heavy chain kinase as determined with synthetic peptides. *J. Biol. Chem.* **265**, 16138-16144.

Brzeska, H., Lynch, T. J., Korn, E. D. (1990b). *Acanthamoeba* myosin I heavy chain kinase is activated by phosphatidylserine-enhanced phosphorylation. *J. Biol. Chem.* **265**, 3591-3594.

Burnside, B. (1978). Thin (actin) and thick (myosinlike) filaments in cone contraction in the Teleost retina. *J. Cell Biol.* **78**, 227-246.

Carboni, J. M., Howe, C. L., West, A. B., Borwick, K. W., Mooseker, M. S., Morrow, J. S. (1988). Characterization of intestinal brush border cytoskeletal proteins of normal and neoplastic human epithelial cells. *Am. J. Pathol.* **129**, 589-600.

Chaitin, M. H., Schneider, B. G., Hall, M. O., Papermaster, D. S. (1984). Actin in the photoreceptor connecting cilium: immunocytochemical localization to the site of outer segment disk formation. *J. Cell Biol,* **99**, 239-247.

Cheney, R. E., Mooseker, M. S. (1992). Unconventional myosins. *Curr. Opin. Cell Biol.* **4**, 27-35.

Cooke, R. (1986). The mechanism of muscle contraction. *CRC Crit. Rev. Biochem.* **21**, 53-118.

Cupples, C. G., Pearlman, R. E. (1986). Isolation and characterization of the actin gene from *Tetrahymena thermophila. Proc Natn. Acad. Sci. USA* **83**, 5160-5164.

Darnell, J., Lodish, H., Baltimore, D. (1990a). Actin, Myosin, and Intermediate Filaments: Cell Movements and Cell Shape. In *Molecular Cell Biology*

(Scientific American Books) pp. 859-902.

Darnell, J., Lodish, H., Baltimore, D. (1990b). Sensory Transduction: The Visual System. In *Molecular Cell Biology* (Scientific American Books) pp. 802-808.

Dentler, W. L., Adams, C. (1992). Flagellar microtubule dynamics in *Chlamydomonas*: cytochalasin D induces periods of microtubule shortening and elongation; and colchicine induces disassembly of the distal, but not the proximal half of the flagellum. *J. Cell Biol.* **117**, 1289-1298.

Detmers, P. A., Goodenough, U., Condeelis, J. (1983). Elongation of the fertilization tube in *Chlamydomonas*: new observations on the core microfilaments and the effect of transient intracellular signals on their structural integrity. *J. Cell Biol.* **97**, 522-532.

Ding, Y., Satir, B. H. (1991). A potential mucous precursor in *Tetrahymena* wild-type and mutant cells. *J. Protozool.* **38**, 613-624.

Doerder, F. P., Debault, L. F. (1975). Cytofluorimetric analysis of nuclear DNA interaction during meiosis, fertilization and macronuclear development in the ciliate *Tetrahymena pyriformis*, syngen I. *J. Cell Sci.* **17**, 471-493.

Drenckhahn, D., Groeschel-Stewart, U. (1977). Localization of myosin and actin in ocular nonmuscle cells. *Cell Tiss. Res.* **181**, 493-503.

Drenckhan, D. Wagner, H. J. (1985). Relation of retinomotor responses and contractile proteins in vertebrate retinas. *Eur. J. Cell Biol.* **37**, 156-168.

Drenckhahn, D., Dermietzel, R. (1988). Organization of the actin filament cytoskeleton in the intestinal brush border: a quantitative and qualitative immunoelectron microscope study. *J. Cell Biol.* **107**, 1037-1048.

Frankel, J. (1989). Ciliate Organization. In *Pattern Formation: Ciliate studies and Models.* (Oxford University Press) pp. 19-41.

Frieden, C. (1982). The Mg^{2+}-induced conformational change in rabbit skeletal muscle G-actin. *J. Biol. Chem.* **257**, 2882-2886.

Fulton, J. F. (1926). The Nature of The Contractile Response of Individual Skeletal Muscle Fibres. In *Muscular Contraction and the Reflex Control of Movement.* (The Williams and Wilkins Company). pp. 3-55.

Gadasi, H., Korn, E. D. (1980). Evidence for differential intracellular localization of the *Acanthamoeba* myosin isoenzymes. *Nature (Lond.).* **286**, 452-456.

Garcia, A., Coudrier, E., Carboni, J., Anderson, J., Vandekerkhove, J., Mooseker, M., Louvard, D., Arpin, M. (1989). Partial deduced sequence of the 110-Kd-calmodulin complex of the avian intestinal microvillus shows that this mechanoenzyme is a member of the myosin I family. *J. Cell Biol.* **109**, 2895-2903.

Garreau de Loubresse, N., Keryer, G., Vigues, B., Beisson, J. (1988). A contractile cytoskeletal network of *Paramecium:* the infraciliary lattice. *J. Cell Sci.* **90**, 351-364.

Garreau de Loubresse, N., Klotz, C., Vigues, B., Ruthin, J., Beisson, J. (1991). Ca^{2+}-binding proteins and contractility of the infraciliary lattice in *Paramecium. Biol. Cell* **71**, 217-225.

Garrels, J. I., Gibson, W. (1976). Identification and characterization of multiple forms of actin. *Cell* **9**, 793-805.

Gavin, R. H. (1976a). The oral apparatus of *Tetrahymena pyriformis* strain WH-6. II. Cytochalasin B inhibition of oral apparatus morphogenesis. *J. Exp. Zool.* **197**, 59-64.

Gavin, R. H. (1976b). The oral apparatus of *Tetrahymena pyriformis* strain WH-6. III. The binding of ^{3}H-cytochalasin B by the isolated oral apparatus. *J. Exp. Zool.* **197**, 65-70.

Gavin, R. H. (1977). The oral apparatus of *Tetrahymena pyriformis* strain WH-6. IV. Observations on the organization of microtubules and filaments in the isolated oral apparatus and the differential effect of potassium chloride on the stability of oral apparatus microtubules. *J. Morph.* **151**, 239-258.

Gavin, R. H. (1980). The oral apparatus of *Tetrahymena.* V. Oral apparatus proteins and their distribution. *J. Cell Sci.* **44**, 317-344.

Gavin, R. H., Duffus, W. A., Contard, P. C. (1989). Characteristics of basal body cartwheel reassembly. *J. Protozool.* **36**, 391-397.

Gibbons, I. R. (1961). The relationship between the fine structure and direction of beat in gill cilia of a lamellibranch mollusc. *J. Biophys. Biochem. Cytol.* **11**, 179-205.

Gibbons, I. R., Grimstone, A. V. (1960). On flagellar structure in certain flagellates. *J. Biophys. Biochem. Cytol.* **7**, 697-716.

Gibbons, I. R., Cosson, M. P., Evans, J. A., Gibbons, B. H., Houck, B., Martinson, K. H., Sale, W. S., Tang, W. Y. (1978). Potent inhibition of dynein adenosinetriphosphatase and of the motility of cilia and sperm flagella by vanadate. *Proc. Natn. Acad. Sci. USA* **75**, 2220-2224.

Glenney, J. R., Glenney, P. (1984). The microvillus 110-kD cytoskeletal protein is an integral membrane protein. *Cell* **37**, 743-751.

Glenney, J. R., Glenney, P. (1985). Comparison of Ca^{2+}-regulated events in the intestinal brush border. *J. Cell Biol.* **100**, 754-763.

Guyton, A. C. (1981a). Neuromuscular Transmission: Function of Smooth Muscle. In *Textbook of Medical Physiology.* (W. B. Saunders Company) pp. 138-148.

Guyton, A. C. (1981b). The Eye: II. Receptor Functions of the Retina. In *Textbook of Medical Physiology.* (W. B. Saunders Co.) pp. 736-747.

Halliburton, W. D. (1887). On muscle-plasma. *J. Physiol.* **8**, 133-202.

Hammer, J. A., Albanesi, J. P., Korn, E. D. (1983). Purification and characterization of a myosin I heavy chain kinase from *Acanthamoeba castellanii. J. Biol. Chem.* **258**, 10168-10175.

Hartwig, J. H., Stossel, T. P. (1979). Cytochalasin B and the structure of actin gels. *J. Mol. Biol.* **134**, 539-553.

Hausman, K. (1978). Extrusion organelles in protists. *Int. Rev. Cytol,* **52**, 197-276.

Hirono, M., Endoh, H., Okada, N., Numata, O., Watanabe, Y. (1987a). *Tetrahymena* actin. Cloning and sequencing of the *Tetrahymena* actin gene and identification of its gene product. *J. Molec. Biol.* **194**, 181-192.

Hirono, M., Nakamura, M., Tsunemoto, M., Yasuda, T., Ohba, H., Numata, O., Watanabe, Y. (1987b). *Tetrahymena* actin: Localization and possible biological roles of actin in *Tetrahymena* cells. *J. Biochem.* **102**, 537-545.

Hirono, M., Kumagai, Y., Numata, O.,Watanabe, Y. (1989). Purification of *Tetrahymena* actin reveals some unusual properties. *Proc. Natn. Acad. Sci. USA* **86**, 75-79.

Hirono, M., Tanaka, R., Watanabe, Y. (1990). *Tetrahymena* actin: Copolymerization with skeletal muscle actin and interactions with muscle actin-binding proteins. *J. Biochem.* **107**, 32-36.

Huang, B., Watterson, D. M., Lee, V. D., Schibler, M. J. (1988). Purification and characterization of a basal body-associated Ca^{2+}-binding protein. *J. Cell Biol.* **107**, 121-131.

Huxley, T. H. (1902). *An Introduction to the Study of Zoology, Illustrated by the Crayfish.* New York (D. Appleton and Company) pp. 181-185.

Jacobsen, G. R., Rosenbusch, J. P. (1976). ATP-binding to a protease-resistant core of actin. *Proc. Natl. Acad. Sci. USA* **73**, 2742-2746.

Jung, G., Korn, E. D., III Hammer, J. A. (1987). The heavy chain of *Acanthamoeba* myosin IB is a fusion of myosin-like and non-myosin-like sequences. *Proc. Natl. Acad. Sci. USA* **84**, 6720-6724.

Kiehart, D. P. (1990). Molecular genetic dissection of myosin heavy chain function. *Cell* **60**, 347-350.

Korn, E. D. (1982) Actin polymerization and its regulation by proteins from nonmuscle cells. *Physiological Reviews* **62**, 672-737.

Korn, E. D., III Hammer, J. A. (1990). Myosin I. *Curr. Op. Cell Biol.* **2**, 57-61.

Korn, E. D., Atkinson, M. A. L., Brzeska, H., III Hammer, J. A., Jung, G., Lynch, T. L. (1988). Structure-function studies on *Acanthamoeba* myosins IA, IB, and II. *J. Cell. Biochem.* **36**, 37-50.

Kuleska-Lipka, D., Baines, I. C., Brzeska, H., Korn, E. D. (1991). Immunolocalization of myosin I heavy chain kinase in *Acanthamoeba castellanii* and binding of purified kinase to isolated plasma membranes. *J. Cell Biol.* **115**, 109-119.

Lackie, J. M. (1986). Motors Based on Actomyosin. In *Cell Movement and Cell Behavior.* (Allen and Unwin).

Laemmli, U. K. (1970). Cleavage of structural proteins during the assembly of the head of bactriophage T4. *Nature* 227, 680-685.

Lemullois, M., Klotz, C., Sandoz, D. (1987). Immunocytochemical localization of myosin during ciliogenesis of quail oviduct. *Eur. J. Cell Biol.* 43, 429-437.

Lowey, S., Slayter, H. S., Weeds, A. G., Baker, H. (1969). Substructure of the myosin molecule. I. Subfragments of myosin by enzymic degradation. *J. Mol. Biol.* 42, 1-29.

Lowey, S., Holt, J. C. (1971). An immunological approach to the interaction of light and heavy chains in myosin. *Cold Spring Harbor Symposium on Quantitative Biology,* Volume XXXVII. 19-28.

Maita, T., Yajima, E., Nagata, S., Takayuki, M., Nakayama, S., Matsuda, G. (1991). The primary structure of skeletal muscle myosin heavy chain: IV. Sequence of the rod, and the complete 1,938-residue sequence of the heavy chain. *J. Biochem.* 110, 75-87.

Maruta, H., Korn, E. D. (1977). *Acanthamoeba* cofactor is a heavy chain kinase required for actin activation of the Mg^{2+}-ATPase activity of *Acanthamoeba* myosin I. *J. Biol. Chem.* 261, 8329-8332.

Matsudaira, P. T., Burgess, D. R. (1979). Identification and organization of the components in the isolated microvillus cytoskeleton. *J. Cell Biol.* 83, 667-673.

Matsudaira, P. T., Burgess, D. R. (1982). Structure and function of the brush border cytoskeleton. In *Cold Spring Harbor Symp. Quant. Biol.* 46, 845-854.

Metenier, G. (1984). Actin in *Tetrahymena paravorax*: ultrastructural localization of HMM-binding filaments in glycinerated cells. *J. Protozool.* 31, 295-215.

Mommaerts, W. F. (1992). Who discovered actin? *Bioessays* 14, 57-59.

Mooseker, M. S., Tilney, L. G. (1975). Organization of an actin filament-

membrane complex: filament polarity and membrane attachment in the microvilli of intestinal epithelial cells. *J. Cell Biol.* **67**, 725-743.

Mooseker, M. S., Bonder, E. M., Grimwade, B. G., Howe, C. L., Keller, T. C. S., Wasserman, R. H., Wharton, K. A. (1982). Regulation of contractility, cytoskeletal structure, and filament assembly in the brush border of intestinal epithelial cells. In *Cold Spring Harbor Symp. Quant. Biol.* **46**, 855-870.

Needham, D. M. (1971). Bringing Muscles into Focus: The First Two Millennia, In *Machina Carnis : The biochemistry of muscular contraction in its historical development.* (Cambridge University Press). pp. 1-26.

Neuhaus, J., Wanger, M., Keiser, T., Wegner, A. (1983). Treadmilling of actin. *J. Mus. Res. Cell Mot.* **4**, 507-527.

Nielsen, E. H. (1990). A filamentous network surrounding secretory granules from mast cells. *J. Cell Sci.* **96**, 43-46.

Peck, R. K., Duborgel, F., Huttenlauch, I., DeHaller, G. (1991). The membrane skeleton of *Pseudomicrothorax* I. Isolation, structure and composition. *J. Cell Sci.* **100**, 693-706.

Philp, N. J., Nachmias, V. T. (1985). Components of the cytoskeleton in the retinal pigmented epithelium of the chick. *J. Cell Biol.* **101**, 358-362.

Pitelka, D. R. (1963). Protozoa as cells. In *Electron Microscopic Structure of Protozoa* (ed. Pergamon Press). pp. 8-70.

Pollard, T. D. (1990). Actin. *Curr. Op. Cell Biol.* **2**, 33-40.

Pollard, T. D., Cooper, J. A. (1986). Actin and Actin-Binding Proteins. A Critical Evaluation of Mechanisms and Functions. *Ann. Rev. Biochem.* **55**, 987-1035.

Pollard, T. D., Korn, E. D. (1973). *Acanthamoeba* myosin I: isolation from *Acanthamoeba castellanii* of an enzyme similar to muscle myosin. *J. Biol. Chem.* **248**, 4682-4690.

Pollard, T. D., Doberstein, S. K., Zot, H. G. (1991). Myosin-I. *Ann. Rev. Physiol.* **53**, 653-681.

Rubenstein, P. A., Spudich, J. A. (1977). Actin microheterogeneity in chick embryo fibroblasts. *Proc. Natl. Acad. Sci. USA* **74**, 120-123.

Salisbury, J. L. (1989). Centrin and the algal flagellar apparatus. *J. Phycol.* **25**, 201-206.

Satir, B. H., Schooley, C., Satir, P. (1973). Membrane fusion in a model system. Mucocyst secretion in *Tetrahymena*. *J. Cell Biol.* **56**, 153-176.

Schliwa, M. (1982). Action of cytochalasin D on cytoskeletal networks. *J. Cell Biol.* **92**, 79-91.

Stossel, T. P., Chaponnier, C., Ezzell, R. M., Hartwig, J. H., Janmey, P. A., Kwiatkowski, D. J., Lind, S. E., Smith, D. B., Southwick, F. S., Yin, H. L., Zaner, K. S. (1985). Nonmuscle actin-binding proteins. *Ann Rev. Cell Biol.* **1**, 353-402.

Szent-Gyorgyi, A. (1948). In *The Nature of Life.* (Academic Press).

Tamm, S., Tamm, S. L. (1988). Development of macrociliary cells in *Beröe*. I. Actin bundles and centriole migration. *J. Cell Sci.* **89**, 67-80.

Tiedtke, A., Gortz, H. D. (1983). Acid phosphatase associated with discharging secretory vesicles (mucocysts) of *Tetrahymena thermophila*. *Eur. J. Cell Biol.* **30**, 254-257.

Tokuyasu, K., Scherbaum, O. (1965). Ultrastructure of mucocysts and pellicle of *Tetrahymena pyriformis*. *J. Cell Biol.* **27**, 67-81.

Towbin, R., Staehlin, T., Gordon, J. (1979). Electrophoretic transfer of proteins from polyacrylamide gels to nitrocellulose sheets: procedure and some applications. *Proc. Nat. Acad. Sci. USA* **76**, 4350-4354.

Vahey, M., Titus, M., Trautwein, R., Scordilis, S. (1982). Tomato actin and myosin: contractile proteins from a higher land plant. *Cell motil.* **2**, 131-148.

Vaughan, D. K., Fisher, S. K. (1987). The distribution of F-actin in cells isolated from vertebrate retinas. *Exp. Eye Res.* **44**, 393-406.

Vigues, B., Metenier, G., Grolier, C. (1984). Biochemical and immunological characterization of the microfibrillar ecto-endoplasmic boundary in the ciliate *Isotricha prostoma*. *Biol. Cell.* **51**, 67-78.

Voet, D., Voet, J. G. (1990). Molecular Physiology. In *Biochemistry.* pp. 1086-1177.

Weeds, A. G. (1969). Light chains of myosin. *Nature* **223**, 1362.

Weeds, A. G., Lowey, S. (1971). Substructure of the myosin molecule II. The light chains of myosin. *J. Mol. Biol.* **61**, 701-725.

Weibel, E. R., Kistler, G. S., Scherle, W. F. (1966). Practical stereological methods for morphometric cytology. *J. Cell Biol.* **30**, 23-38.

Williams, D. S., Linberg, K. A., Vaughan, D. K., Fariss, R. N., Fisher, S. K. (1988). Disruption of microfilament organization and deregulation of disk membrane morphogenesis by cytochalasin D in rod and cone photoreceptors. *J. Comp. Neurol.* **272**, 161-176.

Williams, N. E. (1986). The nature and organization of filaments in the oral apparatus of *Tetrahymena. J. Protozool.* **33**, 352-358.

Williams, D. S., Hallett, M. A., Arikawa, K. (1992). Association of myosin with the connecting cilium of rod photoreceptors. *J. Cell Sci.* **103**, 183-190.

Wolfe, J. (1967). Structural aspects of amitosis: a light and electron microscope study of the isolated macronuclei of *Paramecium aurelia* and *Tetrahymena pyriformis. Chromosoma (Berl.).* **23**, 59-79.

Wolfe, J. (1970). Structural analysis of basal bodies of the isolated oral apparatus of *Tetrahymena pyriformis. J. Cell Sci.* **6**, 670-700.

Wolfe, J. (1980). A possible skeletal substructure of the macronucleus of *Tetrahymena. J. Cell Biol,* **84**, 160-171.

Wolfe, J. (1988). Analysis of *Tetrahymena* mucocyst material with lectins and Alcian Blue. *J. Protozool.* **35**, 46-51.

Wolfe, S. L. (1993). Microfilaments and Microfilament-Based Cell Motility. In *Molecular and Cellular Biology.* (Wadsworth Publishing Company).